An ER surface retrieval pathway safe-guards the import of mitochondrial membrane proteins in yeast

Katja G. Hansen[1#], Naama Aviram[2,3#], Janina Laborenz[1], Chen Bibi[2], Maren Meyer[1], Anne Spang[4], Maya Schuldiner[2*], Johannes M. Herrmann[1*]

1, Cell Biology, University of Kaiserslautern, Germany

2, Department of Molecular Genetics, Weizmann Institute of Science, Israel

3, Current address: Laboratory of Bacteriology, The Rockefeller University, New York, USA

4, Biozentrum, University of Basel, Switzerland

# both authors contributed equally to this study

* Corresponding authors: Johannes M. Herrmann, Cell Biology, University of Kaiserslautern, Erwin-Schrödinger-Strasse 13, 67663 Kaiserslautern, Germany, hannes.herrmann@biologie.uni-kl.de; Maya Schuldiner, Department of Molecular Genetics, Weizmann Institute of Science, Rehovot 7610001, Israel, maya.schuldiner@weizmann.ac.il

One Sentence Summary: The ER surface plays an active role in the productive targeting of membrane proteins to mitochondria

Keywords: Cytosolic chaperones; endoplasmic reticulum; mitochondria; mitochondrial membrane proteins; productive protein targeting; protein import

Abstract

The majority of organellar proteins are translated on cytosolic ribosomes and must be sorted correctly to function. Targeting routes have been identified for organelles such as peroxisomes and the endoplasmic reticulum (ER). However, little is known about the initial steps of targeting of mitochondrial proteins. Here we used a genome-wide screen in yeast and identified factors critical for the intracellular sorting of the mitochondrial inner membrane protein Oxa1. The screen uncovered an unexpected path for targeting of mitochondrial membrane proteins which we termed ER-SURF. This pathway retrieves mitochondrial proteins from the ER surface and re-routes them to mitochondria with the aid of the ER localized chaperone Djp1. Hence, cells use the expanse of the ER surfaces as a fail-safe to maximize productive mitochondrial protein targeting.

Despite detailed understanding of the translocation routes into mitochondria, little is known about cytosolic targeting of mitochondrial precursors (*1, 2*). To identify factors that take part in early targeting steps of mitochondrial membrane proteins, we designed a genetic screen in yeast, monitoring the cytosolic accumulation of non-imported mitochondrial precursors. To this end, we integrated the coding sequence of orotidine-phosphate decarboxylase (Ura3) into the C-terminus of the nuclear encoded inner membrane protein Oxa1, while maintaining the endogenous flanking regions of the *OXA1* gene (Fig. 1A). The corresponding Oxa1-Ura3 protein, expressed in the absence or presence of endogenous Oxa1, was efficiently targeted to mitochondria, integrated into the inner membrane, and fully functional (Fig. 1B, S1A-D). Due to efficient targeting of Oxa1-Ura3 to mitochondria, Ura3 was sequestered from the cytosol, causing a severe growth defect on media lacking uracil. This effect was reverted when the presequence of Oxa1-Ura3 was deleted (ΔN-Oxa1-Ura3), causing its cytosolic accumulation and subsequent uracil-independent growth (Fig. 1C). Hence, a defect in mitochondrial targeting could be monitored by growth on medium lacking uracil.

Using automated mating approaches, the Oxa1-Ura3 construct was introduced into yeast libraries covering 4916 deletion mutants of non-essential genes as well as 1102 DAmP (decreased abundance by mRNA perturbation) mutants of essential genes (*3*) (Fig. 1D). Twelve mutants displayed particularly strong growth on uracil deficient media, suggesting critical roles of corresponding proteins in preventing cytosolic accumulation of the Oxa1-Ura3 precursor (Fig. 1E). While some of the identified factors were expected (e.g. Tim50, an essential subunit of the TIM23 translocase), several of the hits were non-mitochondrial proteins for which a role in mitochondrial protein import or precursor quality control was unknown. These include the uncharacterized proteins Yil029c, Ylr050c and Ycr100c, which we named Ema17, Ema19 and Ema35, respectively (for Efficient Mitochondria Targeting Associated proteins). These three components are predicted to be membrane proteins but were not previously found in mitochondria (*4*). Ema19 is embedded in the ER membrane and conserved among eukaryotes. Deletion mutants lacking Ema19 or Ema35 showed respiration problems at elevated temperatures (Fig. S2A-E).

One of the identified components was Djp1, an abundant yet poorly characterized member of the J-protein/Hsp40 cochaperone family (*5*). Oxa1-Ura3 growth assays with strains lacking other J-proteins confirmed a specific role for Djp1 (Fig. S3A-E). Djp1 is involved in peroxisomal import and the biogenesis of the mitochondrial outer membrane protein Mim1, however the mechanism of its function was not elucidated (*6, 7*). The robust growth of the Oxa1-Ura3-expressing *Δdjp1* mutant in the absence of uracil suggests that Djp1 plays a role in targeting or import of Oxa1 (Fig. 2A). Indeed, in *Δdjp1* cells we observed reduced levels of endogenous Oxa1 and a strong accumulation of the precursor when Oxa1 was overexpressed (Fig. 2B, C, S4A). The relevance of Djp1 was not restricted to Oxa1. The steady state levels of multiple mitochondrial proteins were considerably reduced in *Δdjp1* cells. Djp1 was particularly important in mutants lacking the mitochondrial preprotein receptors Tom70/71(*6*) (Fig. 2C, S4B, C). However, in vitro, we did not observe a considerably reduced Oxa1 import efficiency of isolated *Δdjp1* mitochondria (Fig. 2D, E). This suggests that Djp1 plays a role in Oxa1 targeting that is upstream of the translocation reaction.

Systematic localization studies previously identified Djp1 as an ER-associated protein (*8*), which we confirmed by fluorescence microscopy (Fig. 2F) and subcellular fractionation (Fig. 2 G-I). In addition, a fraction of Djp1 was present in the cytosol where it did not appear to interact with ribosomes (Fig. S5A). We could not exclude that a small fraction of Djp1 may be bound to mitochondria. The ER-binding of Djp1 was very tight, nucleotide-independent and also observed in mutants lacking Ema19 or Ema35, although it appeared to be reduced in these mutants (Fig. S5B-E).

Why would an ER protein affect mitochondrial targeting? A fraction of Oxa1-GFP was ER-localized in *Δdjp1* but not in wild type cells (Fig. 3A). This fraction considerably increased upon depletion of Cdc48, a component crucial for the proteasomal degradation of aberrant ER-associated proteins. Accordingly, Oxa1 lacking its mitochondrial presequence (ΔN-Oxa1) was partially glycosylated (Fig. S6A). Glycosylated Oxa1 was also observed upon overexpression of Oxa1, particularly in *Δdjp1* cells. This suggests that in *Δdjp1* cells, a fraction of Oxa1 that accumulates on the ER surface gets integrated into the membrane, glycosylated and recognized as mislocalized.

Because Djp1 is present at different cellular locations, we tested whether the ER-bound Djp1 is critical for Oxa1 biogenesis: we expressed Djp1-GFP in the presence of GFP-binding chromobody traps that restricted Djp1 either to the ER (Erg11-binder) or to the vacuole (Vph1-binder) (Fig. 3B, S6B-D). The ER-tethered Djp1 version but not that on the vacuolar membrane fully promoted Oxa1 import into mitochondria (Fig. 3C-E). In the absence of Djp1, Oxa1 may insert into the ER membrane, is glycosylated, becomes recognized as aberrant and degraded (Fig. S6E).

In vitro binding experiments showed that the ER surface binds Oxa1 precursor in a Djp1-mediated manner (Fig. 3F, S7A-D). It has previously been assumed that any targeting of mitochondrial proteins to the ER would be a dead-end, resulting in recognition of mistargeting and degradation. However, our results suggest that the association with the ER surface could instead be an intermediate in productive protein targeting to mitochondria. To test whether the ER-localized Oxa1 is imported into mitochondria, we tethered Oxa1 mRNA to the ER surface such that all Oxa1 was translated on ER membranes (*9*). Under these conditions, Djp1 became critical for respiration competence, indicating a crucial role in the productive Oxa1 transfer from the ER to mitochondria (Fig. S7E, F).

In order to investigate mitochondrial import of Oxa1 in a more physiological environment, we employed semi-intact cells having permeabilized plasma membranes (*10*) (Fig. 4A). The in vitro import into semi-intact cells was similar to the import into isolated mitochondria requiring mitochondrial membrane potential and mitochondrial translocases (Fig. S8A-C). However, in semi-intact cells the mitochondrial import of Oxa1 and other mitochondrial membrane proteins was considerably less efficient in the absence of Djp1 (Fig. 4B, C, S8D-F). Preloading of *Δdjp1* semi-intact cells with purified Djp1 restored their competence to import Oxa1 (Fig. S8J). Oxa1 import was almost fully blocked in semi-intact *Δtom70*/*71*/*Δdjp1* cells, indicating that Djp1 and Tom70 cooperate (Fig. S8A, B).

In vitro Djp1 significantly stimulated the import of ER-bound mitochondrial precursors, including that of Oxa1. Hence, Djp1 and other ER proteins maintained precursors import-competent (Fig. 4D-G, S8G). Djp1 was particularly critical for the microsome-to-mitochondria transfer of the very hydrophobic inner membrane protein Coq2 (Fig. S8H), which showed a profound ER association in

Δdjp1 cells (Fig. S8I). When we co-incubated wild type and *Δdjp1* microsomes with low, rate-limiting amounts of mitochondria, a strong Djp1-dependent stimulation of the Oxa1 import was observed (Fig. 4H, I, arrows). Thus, the ER supports import into mitochondria rather than competes with it. In this reaction, we observed a direct binding of Oxa1 precursors to Djp1, particularly when the mitochondrial membrane potential was depleted (Fig. 4J).

Taken together, Oxa1 precursor was found to absorb onto but not to translocate into microsomes from where it was transferred to mitochondria in a Djp1-stimulated reaction (Fig. S9A-C). Soluble translocation intermediates of Oxa1 were not observed in this process, nor did mutation of the HPD motif in the J domain of Djp1 compromise its function (Fig. S9D-G).

The early stages of mitochondrial preprotein targeting are poorly understood. Cytosolic chaperones (*11, 12*) and stabilizing factors called ubiquilins (*13*) associate with mitochondrial preproteins to prevent precursor-mediated proteotoxic stress (*14, 15*). Here we found that the ER surface can function as a capture net to salvage and redirect mitochondrial precursors and thus facilitate early targeting reactions by an import route which we termed ER-SURF pathway (for ER SURFace-mediated protein targeting, Fig. 4K). In consistence, a previous study using a comprehensive proximity-based ribosome profiling approach reported many mitochondrial membrane proteins to be preferentially synthesized on the ER surface (*2*). The conservation and importance of Ema19 in this pathway (Fig. S8K, L) suggests that this re-routing mechanism may be conserved among eukaryotes, including humans.

Hydrophobic mitochondrial proteins were previously observed on the ER, which was interpreted as mislocalization (*16-19*). However, our observations suggest that the ER surface can serve as a safe-guard in targeting of mitochondrial precursor proteins, from where they are retrieved in a Djp1-mediated reaction. This ER-SURF targeting pathway could explain the difficulty in identifying targeting factors for mitochondrial proteins.

References and Notes

1. A. Chacinska, C. M. Koehler, D. Milenkovic, T. Lithgow, N. Pfanner, Importing mitochondrial proteins: machineries and mechanisms. *Cell* **138**, 628-644 (2009).
2. C. C. Williams, C. H. Jan, J. S. Weissman, Targeting and plasticity of mitochondrial proteins revealed by proximity-specific ribosome profiling. *Science* **346**, 748-751 (2014).
3. M. Schuldiner *et al.*, Exploration of the function and organization of the yeast early secretory pathway through an epistatic miniarray profile. *Cell* **123**, 507-519 (2005).
4. M. Morgenstern *et al.*, Definition of a High-Confidence Mitochondrial Proteome at Quantitative Scale. *Cell Rep* **19**, 2836-2852 (2017).
5. C. Sahi, E. A. Craig, Network of general and specialty J protein chaperones of the yeast cytosol. *Proc Natl Acad Sci U S A* **104**, 7163-7168 (2007).
6. D. Papic *et al.*, The role of Djp1 in import of the mitochondrial protein Mim1 demonstrates specificity between a cochaperone and its substrate protein. *Mol Cell Biol* **33**, 4083-4094 (2013).
7. E. H. Hettema *et al.*, The cytosolic DnaJ-like protein djp1p is involved specifically in peroxisomal protein import. *J Cell Biol* **142**, 421-434 (1998).
8. J. L. Koh *et al.*, CYCLoPs: A Comprehensive Database Constructed from Automated Analysis of Protein Abundance and Subcellular Localization Patterns in Saccharomyces cerevisiae. *G3 (Bethesda)* **5**, 1223-1232 (2015).
9. D. Zabezhinsky, B. Slobodin, D. Rapaport, J. E. Gerst, An Essential Role for COPI in mRNA Localization to Mitochondria and Mitochondrial Function. *Cell Rep* **15**, 540-549 (2016).
10. G. Schlenstedt, E. Hurt, V. Doye, P. A. Silver, Reconstitution of nuclear protein transport with semi-intact yeast cells. *J Cell Biol* **123**, 785-798 (1993).
11. R. J. Deshaies, B. D. Koch, M. Werner-Washburne, E. A. Craig, R. Schekman, A subfamily of stress proteins facilitates translocation of secretory and mitochondrial precursor polypeptides. *Nature* **332**, 800-805 (1988).
12. J. C. Young, N. J. Hoogenraad, F. U. Hartl, Molecular chaperones Hsp90 and Hsp70 deliver preproteins to the mitochondrial import receptor Tom70. *Cell* **112**, 41-50 (2003).
13. E. Itakura *et al.*, Ubiquilins Chaperone and Triage Mitochondrial Membrane Proteins for Degradation. *Mol Cell* **63**, 21-33 (2016).
14. L. Wrobel *et al.*, Mistargeted mitochondrial proteins activate a proteostatic response in the cytosol. *Nature* **524**, 485-488 (2015).
15. H. Weidberg, A. Amon, MitoCPR-A surveillance pathway that protects mitochondria in response to protein import stress. *Science* **360**, (2018).
16. Y. C. Chen *et al.*, Msp1/ATAD1 maintains mitochondrial function by facilitating the degradation of mislocalized tail-anchored proteins. *EMBO J* **33**, 1548-1564 (2014).
17. V. Okreglak, P. Walter, The conserved AAA-ATPase Msp1 confers organelle specificity to tail-anchored proteins. *Proc Natl Acad Sci U S A* **111**, 8019-8024 (2014).
18. M. Gamerdinger, M. A. Hanebuth, T. Frickey, E. Deuerling, The principle of antagonism ensures protein targeting specificity at the endoplasmic reticulum. *Science* **348**, 201-207 (2015).
19. E. A. Costa, K. Subramanian, J. Nunnari, J. S. Weissman, Defining the physiological role of SRP in protein-targeting efficiency and specificity. *Science* **359**, 689-692 (2018).

Acknowledgements: We thank Felix Boos, Martin Jung, Einat Zalckvar, Florian Wollweber, Martin van der Laan, Sven Lang and Sabine Knaus for help with experiments, to Ralf Erdmann, Jeffrey Gerst, Sabine Rospert, Doron Rapaport, Roland Wedlich-Söldner for reagents.

Funding: This study was supported by the Deutsche Forschungsgemeinschaft (DIP MitoBalance, SCHU2585/1-1, SFB1190, HE2803/8-2 to M.S. and J.M.H.), BioComp (to J.M.H.) and the Schweizerischer Nationalfond (310030B_163480 to A.S.). M.S is an Incumbent of the Dr. Gilbert Omenn and Martha Darling Professorial Chair in Molecular Genetics.

Author contributions: K.G.H., N.A., M.S. and J.M.H. conceived the project. K.G.H., N.A., J.L. and M.M. designed, performed and analyzed experiments. K.G.H set up the Oxa1-Ura3 screen. K.G.H. and N.A. performed the SGA analysis. N.A. carried out microscopy experiments. K.G.H. performed biochemical experiments, to which also J.L. and M.M. contributed. K.G.H., N.A., M.S. and J.M.H. analyzed data. K.G.H., M.S. and J.M.H. wrote the manuscript with contributions from all authors.

Supplementary Materials

Materials and Methods
Figs. S1 to S9
References *(20-28)*

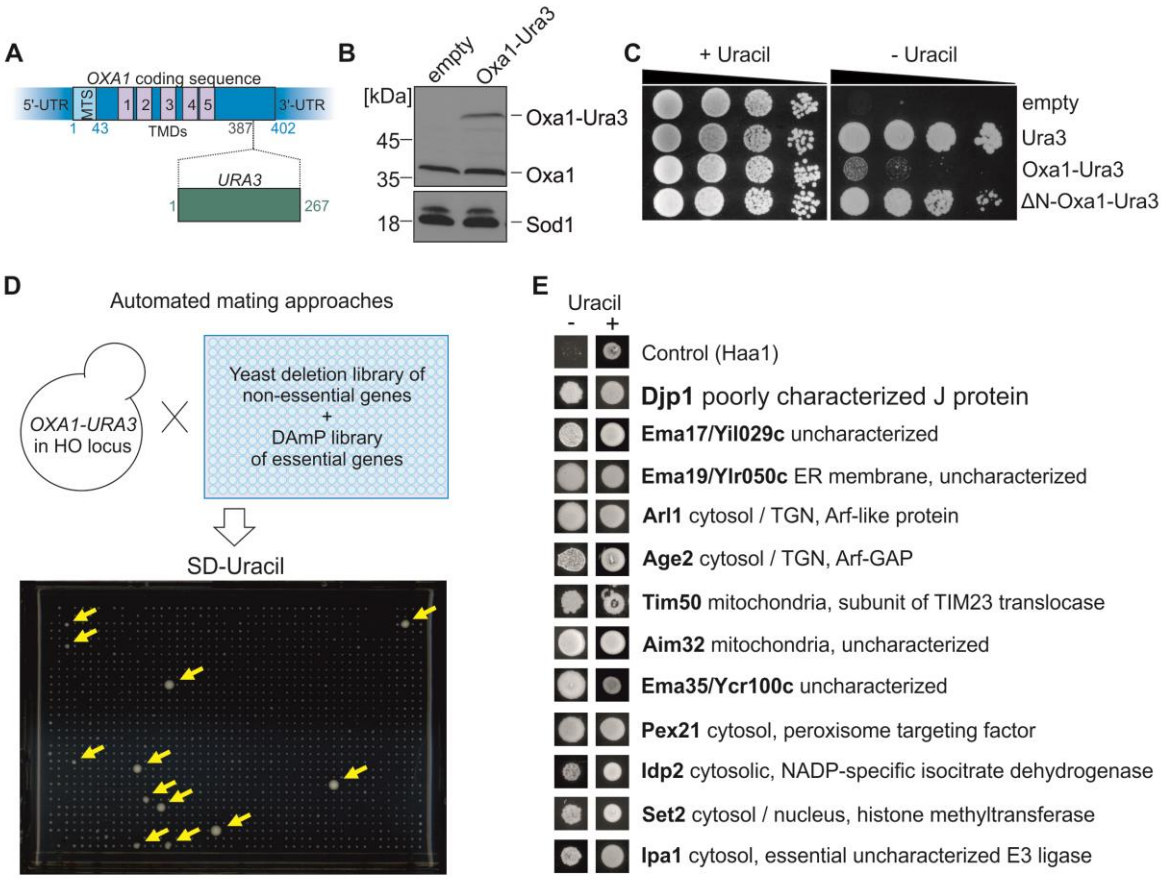

Fig. 1. Genetic screen for mutants that accumulate Oxa1-Ura3 in the cytosol. (**A**) Structure of the Oxa1-Ura3 construct. TMD, transmembrane domain. (**B**) Immune blot of Oxa1-Ura3. (**C**) Growth of *Δura3* mutants expressing the indicated constructs. (**D**) Representative array plate on uracil-deficient medium. (**E**) Proteins critical for the prevention of cytosolic accumulation of Oxa1-Ura3. TGN, trans Golgi network.

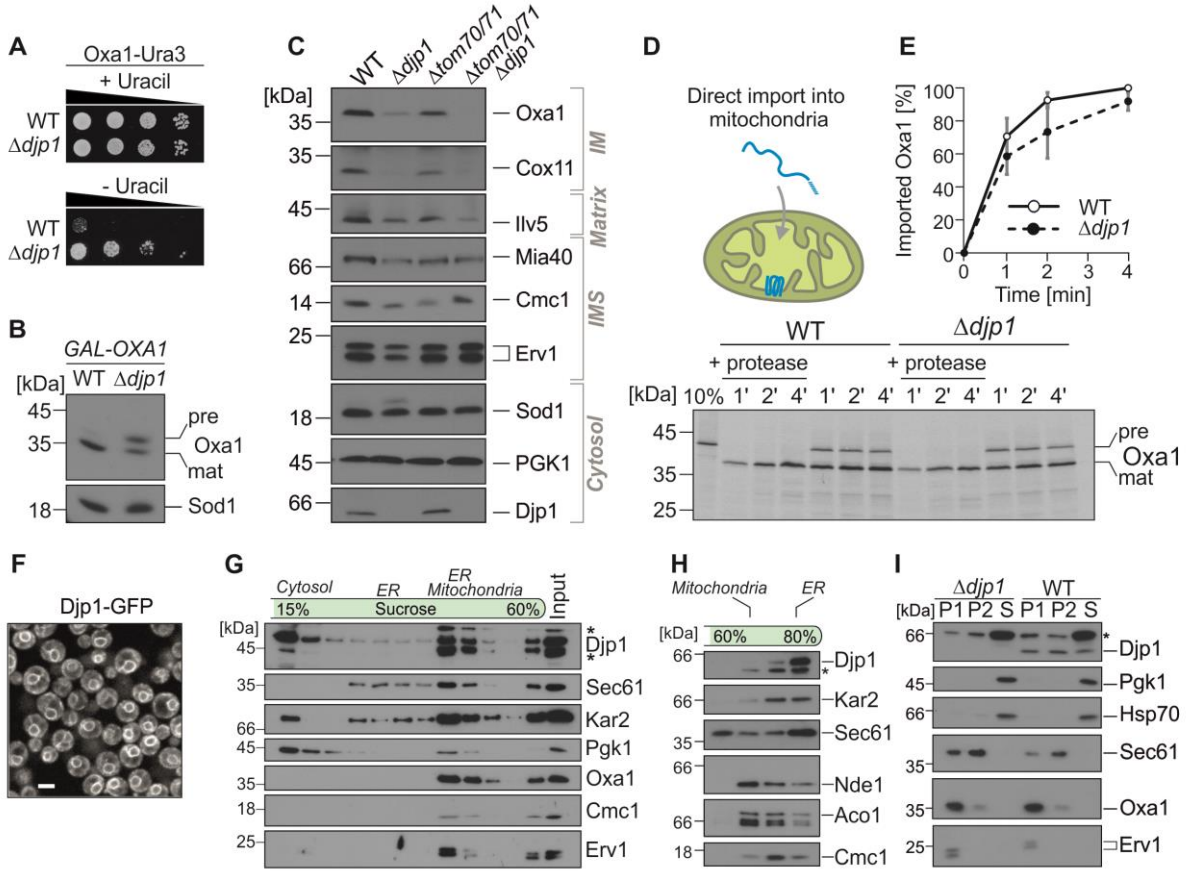

Fig. 2. Djp1 is critical for mitochondrial biogenesis. (**A**) Growth on synthetic medium with or without uracil. (**B**) Oxa1 was overexpressed in wild type (WT) and *Δdjp1* using the GAL-promoter. Cell extracts were analyzed by immune blot; pre, precursor; mat, mature. (**C**) Cellular extracts were analyzed by immune blotting. (**D**, **E**) Radiolabeled Oxa1 precursor (pre) was incubated with WT or *Δdjp1* mitochondria. Data shown are means ± standard deviation, n=4. (**F**) Djp1-GFP shows a perinuclear staining typical for ER proteins. Scale bars, 5 µm. (**G-I**) Cell extracts were separated on sucrose gradients or by differential centrifugation. A large fraction of Djp1 cofractionates with ER membranes. 12,000 and 30,000 *x g* pellets are labeled as P1 and P2, respectively. S, supernatant. Asterisks indicate crossreactions of antibodies.

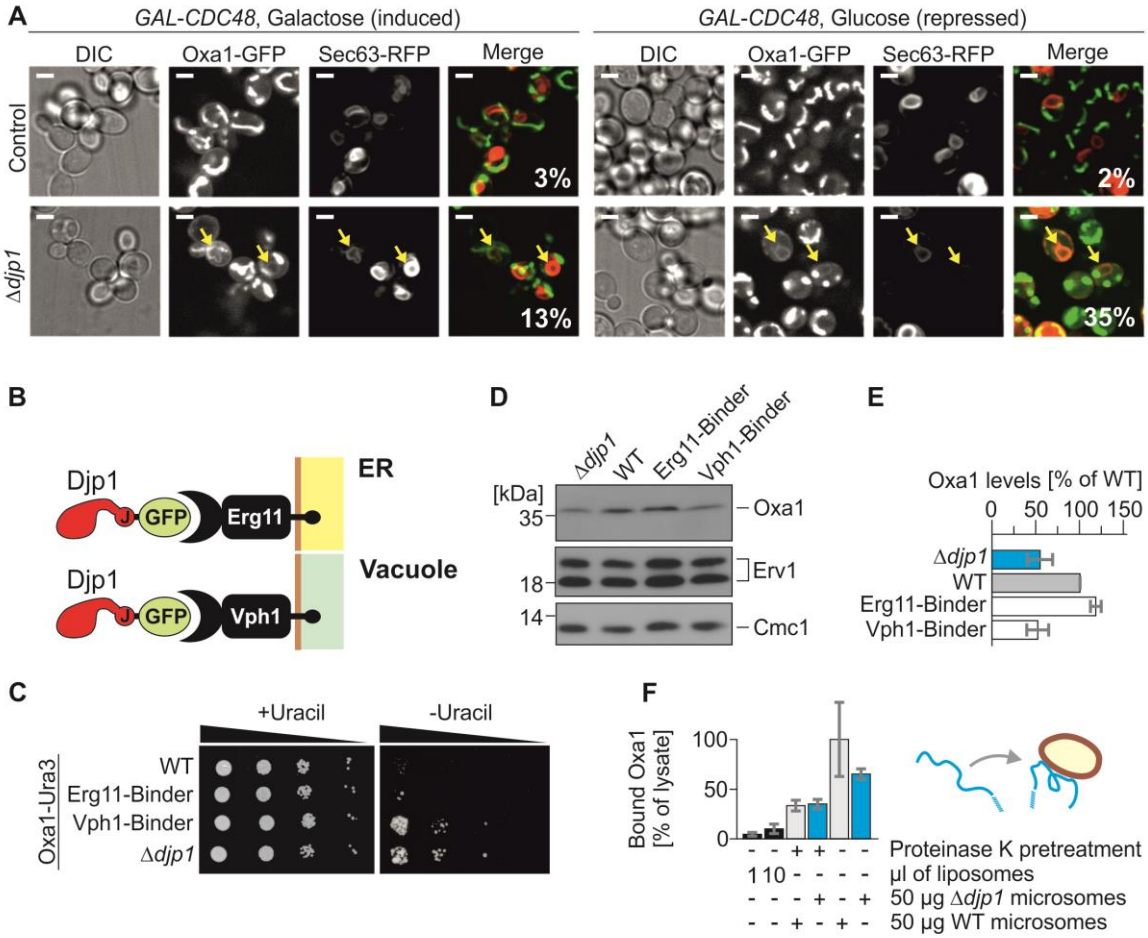

Fig. 3. Djp1 prevents the accumulation of Oxa1 on the ER. (**A**) In the absence of Djp1, Oxa1 partially accumulated on the ER, especially upon depletion of Cdc48. Sec63-RFP served as ER marker. The percentage of cells showing ER-localized Oxa1 is depicted. Scale bars, 5 µm. (**B**) Chromobody-based binders to trap Djp1 on the ER or the vacuole. (**C-E**) ER-localized Djp1 promotes Oxa1-Ura3 efficient import into mitochondria and leads to WT levels of Oxa1. Data show means ± standard deviations, n=3. (**F**) Oxa1 precursor was incubated with liposomes or protease-treated and untreated microsomes. Membranes were reisolated and the associated Oxa1 was quantified. The bound Oxa1 was normalized to the WT microsome sample. Shown are the means ± standard error, n=3.

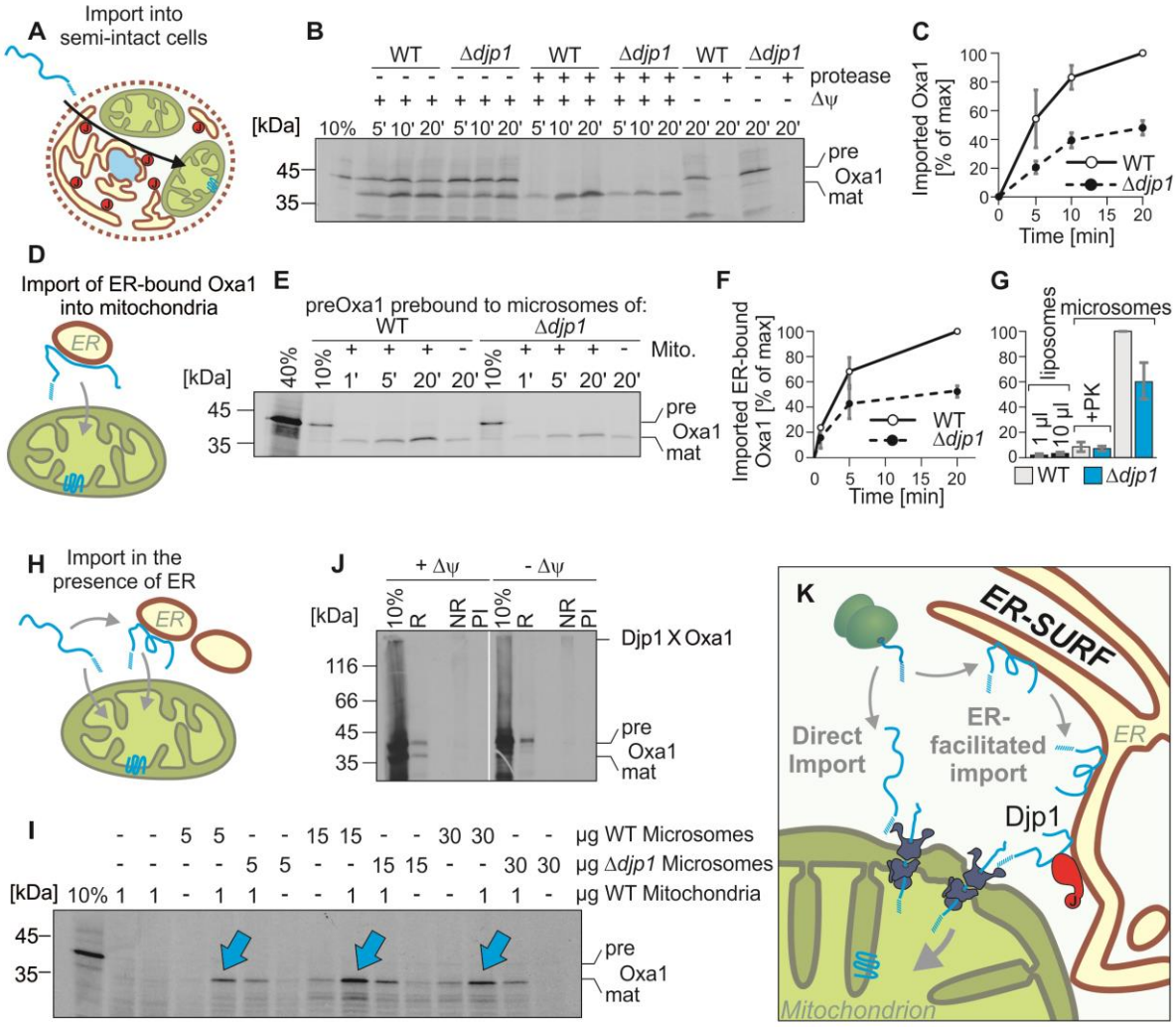

Fig. 4. The ER facilitates Oxa1 import in a Djp1-dependent process. (**A**-**C**) Import of radiolabeled Oxa1 precursor into semi-intact cells. Amounts of protease-resistant mature Oxa1 were quantified. Data shown are means ± standard deviations, n=4. (**D**-**G**) Djp1 promotes the import of ER-bound Oxa1. Quantification shows means ± standard deviations, n=3. (**G**) Microsomes can hand over Oxa1 to mitochondria. Graph shows means ± standard error, n=3. (**H**, **I**) Radiolabeled Oxa1 was incubated with WT and *Δdjp1* microsomes to which low (rate-limiting) amounts of WT mitochondria were added. Non-imported Oxa1 was removed by protease. (**J**) Radiolabeled Oxa1 precursor was incubated with semi-intact cells. After crosslinking with 400 µM DSP, Djp1 was immune-precipitated. NR, non-reducing. R, reducing, i. e. crosslinks were broken. PI: preimmune serum. (**K**) Mitochondria can import Oxa1 precursor directly. However, in vivo, a fraction of Oxa1 associates with the ER surface. The ER-SURF pathway maintains the Oxa1 precursor import-competent and facilitates its re-routing to mitochondria in a Djp1-dependent reaction.

Science
AAAS

Supplementary Materials for

An ER surface retrieval pathway safe-guards the import of mitochondrial membrane proteins in yeast

Katja G. Hansen[#], Naama Aviram[#], Janina Laborenz, Chen Bibi, Maren Meyer, Anne Spang, Maya Schuldiner[*], Johannes M. Herrmann[*]

Correspondence to: maya.schuldiner@weizmann.ac.il; hannes.herrmann@biologie.uni-kl.de

This PDF file includes:

Materials and Methods

Yeast strains

The reporter was introduced into YMS721 (*his3Δ1 leu2Δ0 met15Δ0 ura3Δ0 can1Δ::STE2pr-spHIS5 lyp1Δ::STE3pr-LEU2* mat α*)* resulting in the following strain: *his3Δ1 leu2Δ0 met15Δ0 ura3Δ0 can1Δ::STE2pr-spHIS5 lyp1Δ::STE3pr-LEU2 HO::Prom$_{OXA1}$-OXA1-URA3-Term$_{OXA1}$-Nat^R* mat α*.* This strain was crossed into deletion libraries or into a DAmP library described in (*20*). To test the involvement of the different J-protein genes, they were deleted in this background resulting in the following genotype: *his3Δ1 leu2Δ0 met15Δ0 ura3Δ0 can1Δ::STE2pr-spHIS5 lyp1Δ::STE3pr-LEU2 HO::Prom$_{OXA1}$-OXA1-URA3-Term$_{OXA1}$-Nat^R Δxxx::Hyg^R* mat α. For the import experiments *DJP1* was deleted in YMS721: *his3Δ1 leu2Δ0 met15Δ0 ura3Δ0 can1Δ::STE2pr-spHIS5 lyp1Δ::STE3pr-LEU2 djp1Δ::Nat^R* mat α. *Δema19* (*his3Δ1 leu2Δ0 met15Δ0 ura3Δ0 can1Δ::STE2pr-spHIS5 lyp1Δ::STE3pr-LEU2 ema19Δ::Nat^R* mat α) and *Δema35* from Euroscarf (*his3Δ1 leu2Δ0 lys2Δ0 ura3Δ0 ema35Δ::Kan^R* mat α) were used for the membrane fractionation experiment, a drop dilution assay and for the import of Oxa1 into semi-intact cells.

Strains used to compare the effect of Djp1, Tom70 and Mim1 (ISY7475, *Δdjp1*, *Δtom70/71*, *Δtom70/71Δdjp1, Δmim1)* were already described in (*6*). The *tim17^{ts}* mutant is described in *(21)*.

To establish the reporter, Oxa1-Ura3 was expressed from a pRS313 plasmid in W303 (*leu2-3,112 trp1-1 can1-100 ura3-1 ade2-1 his3-11,15* mat a) or in *Δoxa1* (*leu2-3,112 trp1-1 can1-100 ura3-1 ade2-1 his3-11,15 oxa1Δ::Kan^R* mat α). Additionally, the plasmid was expressed in BY4742 (*his3Δ1 leu2Δ0 lys2Δ0 ura3Δ0* mat α), *Δdjp1* (*his3Δ1 leu2Δ0 lys2Δ0 ura3Δ0 djp1Δ::Kan^R* mat α), *Δydj1* (*his3Δ1 leu2Δ0 lys2Δ0 ura3Δ0 ydj1Δ::Kan^R* mat α), *Δydj1Δdjp1* (*his3Δ1 leu2Δ0 lys2Δ0 ura3Δ0 ydj1Δ::Kan^R djp1Δ::Nat^R* mat α) *Δmmm1* (*his3Δ1 leu2Δ0 lys2Δ0 ura3Δ0 mmm1Δ::Kan^R* mat α) and *Δmdm12* (*his3Δ1 leu2Δ0 lys2Δ0 ura3Δ0 mdm12Δ::Kan^R* mat α) for further confirmation of the growth phenotype.

For microscopy, strains were generated in a BY4741 background (*his3Δ1 leu2Δ0 met15Δ0 ura3Δ0*) as followed: *GAL-CDC48* (*his3Δ1 leu2Δ0 met15Δ0 ura3Δ0 ΔHO::Nat^R Oxa1-GFP::HIS Galp-cdc48::Kan^R* mat a), *GAL-CDC48/Δdjp1 (his3Δ1 leu2Δ0 met15Δ0 ura3Δ0 Δdjp1::Nat^R Oxa1-GFP::HIS Galp-cdc48::Kan^R* mat a*)* and Djp1-GFP (*his3Δ1 leu2Δ0 met15Δ0 ura3Δ0 DJP1-GFP::HIS* mat a). pRS426-Sec63-RFP was transformed into the *GAL-CDC48* strains. Ema19, Ema17 and Ema35 were deleted with a *natNT2* cassette in the background of Djp1-GFP (*his3Δ1 leu2Δ0 met15Δ0 ura3Δ0 DJP1-GFP::HIS Δema::Nat^R* mat a). For the immuno-fluorescence microscopy Djp1-HA (*his3Δ1 leu2Δ0 met15Δ0 ura3Δ0 can1Δ::STE2pr-spHIS5 lyp1Δ::STE3pr-LEU2 DJP1::DJP1-HA-HIS3* mat α) and Djp1^{AAA}-HA (*his3Δ1 leu2Δ0 met15Δ0 ura3Δ0 can1Δ::STE2pr-spHIS5 lyp1Δ::STE3pr-LEU2 DJP1::DJP1^{AAA}-HA-HIS3* mat α) were integrated into the genome of YMS721.

For specific membrane targeting, a chromobody with a *Hyg^R* cassette was genomically integrated into the Djp1-GFP background to create C-terminally tagged fusion proteins, *i.e.* Erg11-chromobody (Erg11-binder), Scm4-chromobody (Scm4-binder) and Vph1-chromobody (Vph1-binder).

Oxa1 protein synthesis was restricted to the ER surface by mRNA trapping at the ER. Therefore, in the background of Oxa1MS (mat a *his3Δ1 leu2Δ0 met15Δ0 ura3Δ0 OXA1::loxP::MS2L::OXA1$_{3'\text{-}UTR}$*) *DJP1* was deleted with *spHIS5* and the strains were transformed with pRS416 or pRS416-Sec63-MCP(x2)-GFP. Oxa1MS and pRS416-Sec63-MCP(x2)-GFP were described in (*9*). To determine the cellular localization of Ema19 a C-terminally (mat a *his3Δ1 leu2Δ0 met15Δ0 ura3Δ0 EMA19-GFP-spHIS5*) or N-terminally GFP-tagged protein was used. N-terminally tagging was achieved using the SWAT-strategy as described in (*22*) *SWAT-NOP1$_{Prom}$-GFP-EMA19 can1Δ::STE2pr-SpHIS5 lyp1Δ::STE3pr-LEU2 his3Δ1 leu2Δ0 met15Δ0* mat *a*.

Automated Mating Approached

The automated mating approaches were performed as previously described (*20*) with the help of a ROTOR HDA Singer robot. The growth was tested on selective media supplemented with or without uracil.

Cloning

The *OXA1* sequence 800 bp upstream of the start codon until 489 bp downstream of the stop codon were cloned into the vector pRS313 using *Xho*I and *BamH*I. By this the 3'-UTR and the 5'-UTR were preserved. Oxa1 exhibits a natural *Eco*RI restriction site in its C terminus. This restriction site was used to introduce the ORF of *URA3* resulting in a fusion protein preserving the whole *OXA1* sequence. For ΔN-Oxa1 and ΔN-Oxa1-Ura3 the sequence corresponding to the amino acid 42 until amino acid 402 (672 for ΔN-Oxa1-Ura3) were amplified.

Downstream of the Oxa1-Ura3 sequence a Nat^R cassette obtained from pFA6a-*NatNT2* was introduced. This construct was used to integrate Oxa1-Ura3 with the endogenous promotor and terminator into the HO locus of the query strain YMS721. The endogenous Oxa1 was preserved to avoid pet phenotypes.For the expression of ΔN-Oxa1 and Oxa1 under a Gal-promotor the ORFs without the stop codon where cloned into pYX223 with the restrictions sites NcoI and SalI resulting in a HA-tagged protein. For site-directed mutagenesis of the HPD motif into AAA Djp1 was subcloned into a pGEM4 vector. The mutated codons were introduced with the help of primers (forward primer: 5'-TATTCAAGAGGCAGCTGCTAAGAATCCCAAT-3'; reverse primer: 5'-ATTGGGATTCTTAGCAGCTGCCTCTTGAATA-3'). After successful mutagenesis $Djp1^{AAA}$ could be subcloned into pYX223 as described for Djp1. The whole ORF of Djp1 with or without a His6-tag was introduced into pYX223 without a stop codon to get HA-tagging with the help of the restrictions sites NcoI and SalI. pYX223-Djp1-HA and pYX223-$Djp1^{AAA}$-HA were used as templates for the integration of Djp1-HA and $Djp1^{AAA}$-HA into the genome.

All deletion mutants were cloned using spHIS5 (pFAa-spHIS5) or NatR (pFA6a-NatNT2). Primer design and protocol were used as described in (*23*).

For heterologous expression of Djp1 in Rosetta2 cells the ORF was cloned into pET19b using NdeI and BamHI.

Isolation of mitochondria

For the isolation of mitochondria cells were grown in full media (1% yeast extract, 2% peptone, pH 5.5) containing 2% galactose as a carbon source and at 30°C. For $tim17^{ts}$ the culture was grown at 25°C and in the morning shifted to 30°C for 3 h. Cells were harvested (4,000 rpm, JA10 Beckmann rotor, 5 min, RT) in the exponential phase. After a washing step, cells were treated 10 min with 2 ml per g wet weight MP1 buffer (10 mM Tris pH unadjusted and 100 mM DTT) at 30°C. After washing with 1.2 M sorbitol, yeast cells were resuspended in 6.7 ml per g wet weight MP2 buffer (20 mM KP_i buffer pH 7.4, 1.2 M sorbitol, 3 mg per g wet weight zymolyase from Seikagaku Biobusiness) and incubated for 1 h at 30°C. Spheroplasts were collected via centrifugation at 4°C and resuspended in ice cold homogenization buffer (13.4 ml/g wet weight) (10 mM Tris pH 7.4, 1 mM EDTA pH 8, 0.2% fatty acids free bovine serum albumin (BSA), 1 mM PMSF, 0.6 M sorbitol). Spheroplasts were disrupted by 10 strokes with a cooled glass potter. Cell debris was removed via centrifugation at 3,300 rpm in a JA10 Beckmann rotor. The

supernatant was centrifuged for 12 min at 10,000 rpm to collect mitochondria. Mitochondria were resuspended in 10 ml of ice cold SH-buffer (0.6 M sorbitol, 20 mM Hepes pH 7.4) and centrifuged again at 4,000 rpm in a JA25.50 Beckmann rotor to remove residual cell debris. To harvest the mitochondria the supernatant was again centrifuged for 12 min at 12,000 rpm. The amount of mitochondria was determined using the Bradford assay.

Isolation of microsomes

For isolation of microsomes (*24*), a 25 ml overnight preculture in full medium containing 2% of glucose as carbon source (YPD) was transferred into 2 l YPD. Cells were grown until OD_{600} between 6 and 7. Cells were harvested (4,000 rpm, 5 min, RT) and resuspended in 6.7 ml/g wet weight EP1 buffer (10 mM DTT, 100 mM Tris pH unadjusted) and incubated shaking for 10 min at RT. After centrifugation the cell pellet was resuspended in 6.7 ml/g wet weight EP2 buffer (0.7 M sorbitol, 0.75x YP, 0.5% glucose, 10 mM Tris pH 7.4, 1 mM DTT, zymolyase 3 mg/g wet weight) and incubated for 1 h at 30°C. Afterwards the suspension was chilled on ice for 2 min and centrifuged at 4°C and 4,000 rpm. Spheroplasts were resuspeded gently in 2x JR Lysis Buffer (0.2 M sorbitol, 50 mM KOAc, 2 mM EDTA, 20 mM Hepes pH 7.4) at about 250 OD/ml. After a centrifugation of 5 min at 10,000 rpm and 4°C, spheroplasts were resuspended in 2x JR Lysis Buffer with 1 mM DTT and 1 mM PMSF at about 500 OD/ml. Spheroplasts were disrupted with 10 strokes of a chilled and motor-driven Teflon on glass douncer at 4°C. Cell debris was removed by centrifugation (3,300 rpm, 4°C, 5 min). Organelles were collected by centrifugation for 10 min and 15,000 rpm in a JA25.50 Beckmann rotor. The pellet containing microsomes was resuspended in B88 (20 mM Hepes pH 6.8, 250 mM sorbitol, 150 mM KOAc, 5 mM $Mg(OAc)_2$) to 2500 OD/ml by gently douncing with 7 strokes in a 10 ml homogenizer. 2 ml of the suspension was loaded on a two-step sucrose gradient (1 ml 1.5 M sucrose in 20 mM Hepes pH 7.4, 50 mM KOAc, 2 mM EDTA and 1 ml of 1.2 M sucrose in 20 mM Hepes pH 7.4, 50 mM KOAc, 2 mM EDTA) and centrifuged for 1 h at 40,000 rpm, 4°C, in a SW60 TI Beckmann swingout rotor. The microsome containing interface was collected with a plastic Pasteur pipette. Microsomes were washed by a 5-fold dilution with B88 and centrifuged again for 10 min at 15,000 rpm in a JA25.50 Beckmann rotor. Microsomes were resuspended in 300 µl to 1 ml B88, depending on pellet size, and with the help of a 10 ml homogenizer. The amount of microsomes was determined using Bradford assay.

Preparation of semi-intact cells

The protocol for the preparation of semi-intact cells was adapeted from *(10)*. Precultures were grown in YPGal at 30°C. *tim17^{ts}* was precultured at 25°C and in the morning set at 30°C for 3 h. Cells were harvested (700 xg, 7 min, RT) in the exponential phase. The cell pellet was resuspended in 25 ml SP1 buffer (10 mM DTT, 100 mM Tris pH unadjusted) and incubated for 10 min at 30°C shaking. After centrifugation (1,000 xg, 5 min, RT) the pellet was resuspended in 6 ml SP2 buffer (0.6 M sorbitol, 1x YP, 0.2% glucose, 50 mM KP_i pH 7.4, 3 mg/g wet weight zymolyase) and incubated at 30°C for maximal 30 min. The spheroplast formation was monitored every 15 min. Spheroplasts were collected and resuspended in 40 ml of SP3 buffer (1x YP, 1% glucose, 0.7 M sorbitol) and incubated for 20 min at 30°C shaking. After centrifugation (1,000 xg, 5 min, 4°C) spheroplasts were washed two times with 20 ml of ice cold permeabilization buffer (20 mM Hepes pH 6.8, 150 mM KOAc, 2 mM $Mg(OAc)_2$, 0.4 M sorbitol). The pellet was resuspended in 1 ml permeabilization buffer containing 0.5 mM EGTA and 100 µl aliquots were slowly frozen over liquid nitrogen for 30 min.

Cytosol preparation

YMS721 or Δ*djp1* were grown in 1 L YPD to an OD_{600} of ~10. Cells were harvested (4,000 rpm, JA10 Beckmann rotor, 5 min, RT) and washed with cold water. After a second centrifugation the yeast cells were washed again with cold water and pelleted (4,000 rpm, JA10 Beckmann rotor, 5 min, 4°C). The pellet was resuspended in 5 ml of ice cold Buffer A (50 mM KOAc, 1 mM $Mg(OAc)_2$, 2 mM DTT, 20 mM Hepes, pH 7.4). The cells were dropped into liquid nitrogen. The resulting pearls were given into a mortar together with liquid nitrogen and kept on ice. The frozen yeast was ground for around 30 min until a powder was achieved. As the cell powder started to melt at room temperature 5 ml of Buffer A containing 2 mM DTT and 2 mM PMSF was added and the thawing process was continued. The lysate was transferred into Beckmann tubes and spun at 9,000 rpm for 10 min at 4°C in a JA-25.50 rotor. The cloudy supernatant was collected, transferred into 50Ti tubes and centrifuged for 35 min at 100,000 xg and 4°C. The supernatant was collected avoiding the top layer containing the lipids and the pellet. The protein amount was determined and the cytosol was aliquoted, frozen in liquid nitrogen and stored at -80°C.

Preparation of liposomes

20 mg phosphatidylcholine (POPC) was dissolved in 1 ml of B88 (20 mM Hepes pH 6.8, 250 mM sorbitol, 150 mM KOAc, 5 mM $Mg(OAc)_2$) by vortexing at maximal speed for 30 min at 4°C. The suspension was frozen in liquid nitrogen, thawed at 40°C and vortexed for 1 min at maximal speed. 10 cycles were performed.

Proteinase K treatment of microsomes

50 µg microsomes in B88 were supplemented with 100 µg/ml proteinase K and incubated for 30 min on ice. The protease was stopped with 2 mM PMSF for 10 min on ice. The microsomes were reisolated by centrifugation (10 min, 30,000 xg, 4°C).

Import into mitochondria

The import was performed as previously described (*25*). For the import of Oxa1 into isolated mitochondria of the *tim17*^{ts} mutant and the WT with or without membrane potential just one time point (2 min at 30°C) was chosen.

For the import of ER-bound proteins, radiolabeled lysate of the respective proteins was added to 50 µg microsomes in B88 and 2 mM ATP and incubated for 2 min at 30°C. Afterwards microsomes were pelleted at 30,000 xg and 4°C for 10 min and the supernatant was removed. The microsomes were resuspended in SH-buffer and a 10% control was taken. The rest was distributed to different prepared reaction mixtures containing either mitochondria in import buffer (500 mM sorbitol, 50 mM Hepes pH 7.4, 80 mM KCl, 10 mM $Mg(OAc)_2$ and 2 mM KH_2PO_4), 2 mM ATP and 2 mM NADH or only into import buffer with ATP and NADH. Mitochondria were energized for 10 min at 30°C before adding Oxa1 bound to microsomes. For the mitochondria containing reaction, samples were taken after 1, 5 and 20 min. Microsomes alone were incubated for 20 min. The import reaction was stopped in a 1:10 dilution of ice cold SH buffer and samples were treated with proteinase K as described above. To test the importance of proteins for the import of membrane-bound Oxa1, 1 or 10 µl of liposomes, proteinase K-treated microsomes and untreated microsomes were incubated with Oxa1 as described above. The

import into mitochondria was performed in presence of 2 mM PMSF to inhibit residual protease. The import was stopped after 20 min.

The in vivo oxidation of the Mia40 substrate Cox19 was analyzed by a pulse-labeling experiment in yeast cells followed by immunoprecipitation as described before (*26*).

Addition of purified Djp1, Djp1^{AAA} and cytosol to the *in vitro* import assay with isolated mitochondria

Oxa1 lysate was preincubated for 5 min with either 0, 2 or 10 µg purified Djp1 or Djp1^{AAA} in the presence or absence of 50 µg cytosol. Energized *Δdjp1* mitochondria were added and Oxa1 was allowed to import for 2 min at 30°C. The import was stopped and the samples were further treated as described before.

Import into Semi-Intact Cells

Semi-intact cells were thawed on ice and the OD_{600} was measured. Semi-intact cells of an OD_{600} 0.2 up to 0.5 were used per reaction. Semi-intact cells were added to a mixture of B88 buffer, 2 mM ATP, 2 mM NADH, 5 mM creatine phosphate and 100 µg/ml creatine phosphatase. Radiolabeled lysate was added and the mixture incubated 10 min on ice to allow the cells to take up the lysate. Afterwards the suspensions were incubated at 30°C. For kinetics samples were taken after 5, 10 or 20 min. The import reaction was stopped in a 1:10 dilution in ice cold B88 buffer and 5.6 µg/ml valinomycin, 44 µg/ml antimycin A and 42.5 µg/ml oligomycin and treated with or without 100 µg/ml proteinase K for 30 min on ice. The protein digestion was stopped by the addition of 2 mM PMSF. Semi-intact cells were centrifuged (4,000 xg, 5 min, 4°C), washed again with B88 and 2 mM PMSF and centrifuged for 10 min at 4,000 xg and 4°C. Finally, the pellet was resuspended in reducing loading buffer.

For the comparison of the five different strains the import was stopped after 10 min.

Oxa1 binding onto microsomes

10 µg microsomes were used per reaction and energized in B88 and 2 mM ATP. 100 µM CCCP were used in some samples to determine the background import of mitochondrial contaminations in the microsomal preparations. Microsomes were incubated for 10 min at 25°C and afterwards radioalabeled Oxa1 was added and incubated for 30 min at 25°C. The import reaction was stopped in a 1:10 dilution with ice cold SH buffer and samples were treated with or without 100 µg/ml proteinase K for 30 min on ice. The digestion was stopped with 2 mM PMSF. After centrifugation (30,000 xg, 4°C, 10 min), the microsomes were washed with SH/KCl buffer (0.6 M sorbitol, 20 mM Hepes pH 7.4, 150 mM KCl) and 2 mM PMSF. Samples were resuspended in reducing loading buffer.

Oxa1 binding onto different membranes

Oxa1 lysate was incubated with liposomes, proteinase K-pretreated or untreated microsomes in B88 supplemented with 2 mM ATP and 2 mM PMSF at 30°C for 2 min. The samples were centrifuged for 10 min at 30,000 xg and 4°C. The supernatant was discarded and the pellet was resuspended in SH-buffer. 10% of the sample was analyzed.

Cycling of Djp1

Oxa1 was prebound to mircosomes as described before. After reisolation of the membranes, microsomes were resuspended in import buffer, 2 mM ATP, 2 mM NADH and 100 µg cytosol was added. The suspension incubated 10 min at 30°C. Microsomes and cytosol were fractionated again by centrifugation (10 min, 30,000 xg, 4°C). The proteins of the supernatant were TCA precipitated and pelleted (20 min, 30,000 xg, 4°C). The pellet was washed with ice cold acetone followed by another centrifugation step (20 min, 30,000 xg, 4°C). The pellet was dried at 30°C and resuspended in reducing loading buffer.

Radiolabeled protein

To prepare ^{35}S-methionine labeled proteins the TNT® Quick Coupled Transcription/Translation Kit from Promega was used.

Cell lysates

For whole cell lysates, yeast strains were cultivated either in full or selective media and an OD 2 was harvested in their exponential growth phase. Cells were washed with water and resuspended in reducing loading buffer. Cells were boiled for 3 min at 96°C and glass beads (0.5 mm) were added. Cells were vortexed for 1 min and boiled again for 5 min. The equal amount of OD 0.2 up to OD 0.4 was loaded on an SDS-gel.

Endo H treatment

Cell lysates were mixed with G5 buffer and with or without 1,000 units of Endo H from New England Biolabs and incubated for 1 h at 37°C. The enzyme was inactivated by boiling for 3 min at 96°C. Biological triplicates were used for the quantification of the glycosylated protein amount.

Growth assays

Yeast strains were grown either in full or selective media and cells were harvested in their exponential phase and washed with sterile water. For growth tests on respiratory media precultures contained galactose as a carbon source.

Growth curves were performed automated in a 96 well plate using the ELx808™ Absorbance Microplate Reader (BioTek®). The growth curves started at OD_{600} 0.1 and the OD_{600} was measured every 10 min for 72 h at 30°C. The mean of technical triplicates was calculated and plotted in R.

For drop dilution assays an OD_{600} of 0.5 was harvested, washed and a serial 1:10 dilution was done. From each dilution 3 µl were dropped on the respective media. The growth was documented after different days.

For the halo assay 100 µl of an OD_{600} 0.01 was distributed on plates and a filter paper was soaked with 10 µl 20 mM CCCP or 10 µl DMSO as a control.

Salt washing of membranes

Crude membranes were taken in SH buffer containing different amounts of NaCl (10 mM up to 1 M) and incubated for 10 min at 25°C. Membranes were spun down and resuspended in reducing loading buffer. The proteins in the supernatant were precipitated with the help of 12% trichloracetic acid (TCA) at -80°C for 2 h. The proteins were pelleted (30,000 xg, 4°C, 20 min) and washed with ice cold acetone. The pellet was dried at 30°C and resuspended in reducing loading buffer.

To test the dependence of Djp1 membrane binding on ATP or ADP, crude membranes were treated with SH buffer containing 2.5 M NaCl supplemented with either 5 mM ATP, ADP or EDTA.

Sucrose Gradient of semi-intact cells to separate mitochondria and ER

Two aliquots of BY4742 semi-intact cells were thawed on ice. Semi-intacts were centrifuged for 5 min at 3,000 xg and 4 °C. The cells were resuspended in 2 ml ice cold SEM buffer (250 mM Sucrose, 1 mM EDTA, 10 mM MOPS-KOH, pH 7.2). The semi-intact cells were homogenized with 10 strokes of a 5 ml glass Teflon potter. 5.5 mg of the homogenate was loaded on top of a sucrose gradient adapted of (*27*) consisting of 1.5 ml 80%, 1.5 ml 60%, 4 ml 32%, 1.5 ml 23% and 1.5 ml 15% sucrose in EM buffer (1 mM EDTA, 10 mM MOPS-KOH, pH 7.2). The gradient was centrifuged for 1 h at 4°C and 134,000 xg in a SW40 Beckmann rotor. 1 ml of each fraction was taken and 50 µl aliquots of each was augmented with 2x concentrated reducing loading buffer. The samples were boiled at 65°C for 3 min and the same volume of each fraction was loaded on a 14/0.2% SDS-gel.

Sucrose Gradient of crude mitochondria to separate mitochondria and ER

Yeast strains were grown either in 2 L YPGal (Djp1^{AAA}-HA) or in 2 L YPD (Erg11-chromobody) until exponential phase and harvested. A mitochondrial isolation was performed as described in (*27*). 5 mg/ml up to 10 mg/ml were loaded onto a sucrose gradient (3 ml 60%, 4 ml 32%, 1.5 ml 23% and 1.5 ml 15% sucrose in EM buffer) and centrifuged for 1 h at 4°C and 134,000 xg in a SW40 Beckmann rotor. 1 ml of each fraction was taken and 50 µl aliquots of each was augmented with 2x concentrated reducing loading buffer. The samples were boiled at 65°C for 3 min and the same volume of each fraction was loaded on a 14/0.2% SDS-gel.

Membrane fractionation assay

Yeast cells were grown to their exponential phase in 20 ml YPD cultures. An OD_{600} of 20 were harvested (5 min, 5,000 xg) and washed with water. Cells were resuspended in 1 ml of MP1 buffer (10 mM Tris pH unadjusted and 100 mM DTT) and incubated for 10 min at 30°C. The cells were pelleted (5 min, 5,000 xg) and washed with 1.2 M sorbitol. The cells were pelleted again and resuspended in 1 ml ice cold homogenization buffer (10 mM Tris pH 7.4, 1 mM EDTA pH 8, 2 mM PMSF, 0.6 M sorbitol, 1 M NaCl). The cells were sonicated for 10 s and centrifuged for 3 min at 5,000 xg and 4°C. The supernatant was transferred into fresh tubes and centrifuged again (3 min, 5,000 xg, 4°C). Again, the supernatant was transferred into a fresh tube to remove cell debris from the lysate (3 min, 5,000 xg, 4°C). The lysate was centrifuged 5 min at 12,000 xg and 4°C. Once again the supernatant was transferred and the pellet (P1) with enriched mitochondria was resuspended in reducing loading buffer. To enrich the ER, the residual supernatant was centrifuged for 30 min at 30,000 xg and 4°C. The proteins of the supernatant (cytosol) were TCA precipitated and the pellet containing the ER membranes (P2) was resuspended in reducing loading buffer. The same volume of each fraction was subjected to SDS-PAGE.

Isolation of 80S ribosomes

100 ml of a culture in exponential growth phase were treated for 10 min with 0.1 mg/ml cycloheximide. Cells were harvested and the cell pellet was resuspended in lysis buffer (0.1 mg/ml cycloheximid, 20 mM Tris pH 8, 140 mM KCl, 12 mM $MgCl_2$, 0.1% NP-40, 1 mM PMSF, 1x protease inhibitor cocktail from Roche). Acid washed beads (0.5 mm diameter) were added and the suspension was vortexed 10 times for 30 s. Cell debris were removed via centrifugation (two times for 10 min at 30,000 xg and 4°C) and the supernatant containing ribosomes and ribosome-associated proteins was loaded on a linear sucrose gradient from 10 to 34%. The sucrose was solved in 40 mM Tris pH 8, 280 mM KCl, 24 mM $MgCl_2$, 0.1 mg/ml cycloheximide and 1x protease inhibitor cocktail. The gradient was centrifuged for 4 h at 4°C and 33,000 rpm in a SW41 Beckmann swing out rotor. 16 fractions were taken and TCA precipitated.

Binding Assay

His_6-Djp1-HA was coupled to Ni-NTA sepharose beads from Amintra in 2x concentrated binding buffer (100 mM NaCl and 20 mM Tris pH 7.4). Ni-NTA beads with no protein bound were washed and also taken up in 2x binding buffer. The beads were equally distributed into 1x binding buffer with different amounts of NaCl (50 mM, 150 mM and 500 mM) or with either 150 mM NaCl, 4 mM ATP and 1 mM $MgCl_2$ or 150 mM NaCl, 4 mM ADP and 1 mM $MgCl_2$. Diluted Oxa1 lysate was added to the mixture and incubated reeling at 4°C for 20 min. The beads were washed 3 times with 1 ml 2x binding buffer and the proteins were eluted with reducing loading buffer and 30 mM EDTA.

Crosslinking and Immunoprecipitation

Oxa1 was imported in presence or absence of VAO buffer (2.2 µg/ml valinomycin, 17.6 µg/ml antimycin A and 17 µg/ml oligomycin) into semi-intact cells for 5 min. 400 µM of DSP in DMSO were added and the mixture was incubated for 20 min at 30°C. The crosslinker was quenched for 5 min with 100 mM glycin. After a washing step with B88, semi-intact cells were resuspended in native lysis buffer (30 mM Tris/HCl pH 8, 100 mM NaCl, 0.1% Tx-100, 5 mM EDTA pH 8, 2 mM PMSF) and incubated reeling at 4°C for 14 min. After a clarifying spin (20 min, 4°C, 20,000 xg) the supernatant was supplemented with activated protein A sepharose beads from Amintra and either Djp1 or preimmune sera and incubated reeling for 1 h at 4°C. The beads were washed (spinning 2 min, 2,000 xg, 4°C) twice with lysis buffer without PMSF and once with 20 mM Tris pH 8. Proteins were eluted using either reducing or non-reducing loading buffer.

Protein purification

Yeast cells expressing either His_6-Djp1-HA or the empty plasmid were precultured in SD media and kept overnight in SGal to express Djp1. Cells were harvested on the next day and spheroplasts produced like it is described for the mitochondria isolation. Spheroplasts were washed with SH buffer and the pellet was resuspended in lysis buffer (100 mM NaCl, 4 mM $MgCl_2$, 20 mM Tris pH 8, 1% Triton X-100, 2 mM PMSF and 1x protease inhibitor cocktail) and incubated for 10 min on ice. After two clarifying spins (15 min, 4°C, 20,000 xg) the supernatant was supplemented with in lysis buffer equilibriated Ni-NTA beads and incubated reeling at 4°C for 1 h. The beads were pelleted (2 min, 4°C, 2,000 xg) and

washed two times with washing buffer A (100 mM NaCl, 20 mM Tris pH 8 and 20 mM imidazole) and twice with washing buffer B (100 mM NaCl, 20 mM Tris pH 8). For elution, the beads were incubated reeling for 5 min at 4°C with elution buffer (25 mM Tris pH 7, 250 mM NaCl, 300 mM imidazole and 500 µM EDTA pH 8).

Peptide spot assay to monitor Djp1 binding

The peptide membrane was washed 2 min with methanol and 2 min with water. Afterwards it was equilibrated for 20 min in binding buffer (20 mM Tris pH 7, 200 mM NaCl). The membrane was incubated 3 h with 1 µM purified Djp1 and washed twice for 10 min with binding buffer and twice with TBS buffer (50 mM Tris, 150 mM NaCl, pH 7.4). The bound proteins were transferred onto a nitrocellulose membrane using the semi-dry immune blot. The bound Djp1 was detected with the HA-antibody from Roche.

Antibodies

If not differently described antibodies were raised in rabbits using recombinant purified proteins. The secondary antibody was ordered from BioRad (Goat Anti-Rabbit IgG (H+L) -HRP Conjugate, #172-1019, Goat Anti-Mouse IgG (H+L)-HRP Conjugate, #172-1011). The antibody against Pgk1 was ordered from Invitrogen (PGK1 Monoclonal Antibody (22C5D8), #459250). The horseradish-peroxidase coupled HA antibody was ordered from Roche (Anti-HA-Peroxidase, High Affinity (3F10), #12 013 819 001).

Fluorescence microscopy

Manual microscopy was performed using VisiScope Confocal Cell Explorer system, composed of a Zeiss Yokogawa spinning disk scanning unit (CSU-W1) coupled with an inverted Olympus IX83 microscope. Images were acquired using a 60× oil lens and captured by a connected PCO-Edge sCMOS camera, controlled by VisView software, with wavelength of 488 nm (GFP) or 561 nm (mCherry/RFP). Images were transferred to Adobe Photoshop CS6 or Fiji for slight adjustments to contrast and brightness.

Data Analysis

Quantifications were done using the ImageQuant GE Healthcare software. Films were scanned and processed in Coral Photopaint X7 and figures assessed in Coral Draw X7. Membranes for immune blots were cut in pieces for decoration with different antibodies. Microscopy pictures were processed in Fiji and figures assessed in Coral Draw X7. Statistical analysis was performed in Excel 2016 to determine the mean, standard deviation or standard error. Graphs were either assessed using R or Excel 2016. The colony size shown in S3B and C were extracted with the help of the Balony Software. Afterwards, the colony sizes were normalized to the growth on YPD and compared to the growth of the negative control Oxa1-Ura3 by a two-tailed students t-test.

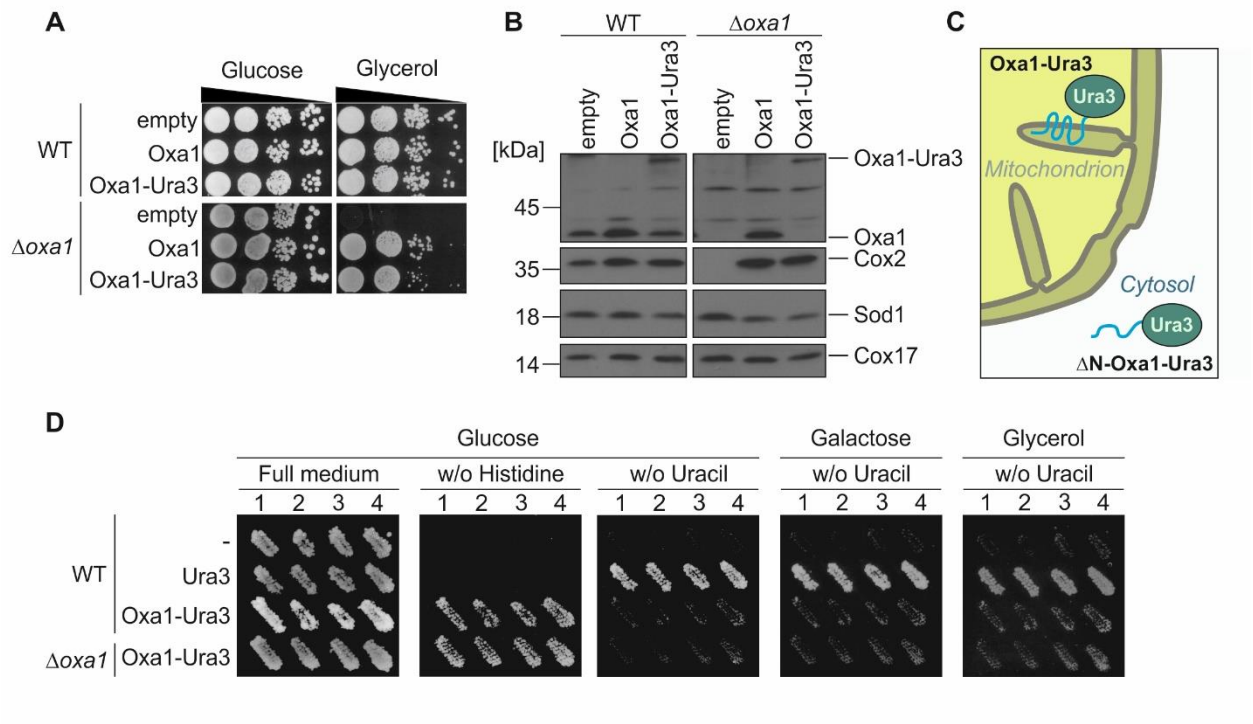

Fig. S1. Oxa1-Ura3 expression fully complements *OXA1* deletion. (A) Oxa1-Ura3 was expressed under the *OXA1* promoter from a single copy plasmid in WT or *Δoxa1* cells. The expression of Oxa1-Ura3 leads to respiratory growth. **(B)** Cell extracts of the different strains were analyzed in immune blots. Cox2 is a mitochondrially encoded inner membrane protein that is degraded in the absence of functional Oxa1. Cox2 levels are comparable in *Δoxa1* expressing Oxa1 or Oxa1-Ura3. **(C)** Predominant cellular location of Oxa1-Ura3 and ΔN-Oxa1-Ura3. The ΔN-Oxa1-Ura3 version which lacks a mitochondrial targeting sequence is located in the cytosol. **(D)** Growth of independently generated mutant isolates. WT and *Δoxa1* strains were transformed with pRS313-Oxa1-Ura3. The WT without any plasmid was used as a negative control. WT cells transformed with pRS316 were used as a positive control. Four colonies of each transformation were picked and analyzed for their ability to grow on uracil-deficient media. The expression of Oxa1-Ura3 does not lead to a strong growth on plates lacking uracil.

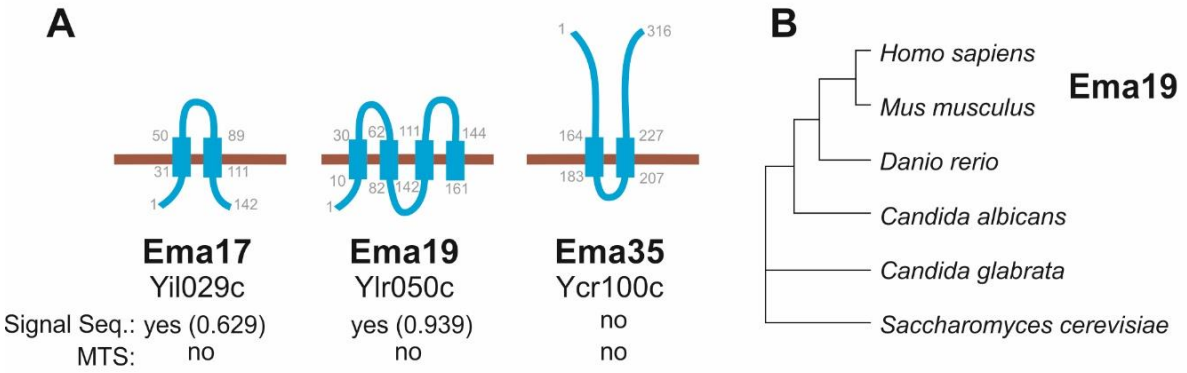

C

```
Sc      ----------------------MKLGHREQQFYLWYFIVHIPITIFIDSSVVIPAKWQL
Cg      ---------------------MISSLSVFEEKFYYYYCLVHIPITVLVDSSVAVPDKWVL
Ca      -------------------------MKLIDKVYLWYFIIHIPITIFIDSSIVIPKQYQL
Hs      -------------------MGAPATRRCVEWLLGLYFLSHIPITLFMDLQAVLPRELYP
Mm      -------------------MGALAARRCVEWLLGLYFVSHIPITLFIDLQAVLPPELYP
Dr      ----------------------MFLRVLEIIYFIYFASHIPITLLVDLQALLPEHVYP
                                     : .   *   *****:::* .  :* .

Sc      GIAQKVVSDHIAKQHDFLLSEKPEWLYWFVVLELVLQLPLFVYFVNKFWNSSE-------
Cg      L--PGLVQWHIRQNNDFLLYEKPMWLQLFVWWELVFQLPLFFYFAHQFKKIWALRSKDTK
Ca      PITKSILEFHISTNNDILLAYPQTWFKIFGFIELIFQLPLFFYFIYKLLSS---------
Hs      VEFRNLLKWYAKEFKDPLLQEPPAWFKSFLFCELVFQLPFFPIATYAFLKGSC-------
Mm      QEFSNLLRWYSKEFKDPLMQEPPVWFKSFLLCELVFQLPFFPIAAYAFFKGSC-------
Dr      PELIKLLHWYAGEFKDPMMMDPPAWFKSFVFCEALVQLPFFPVAAYAFLKGGC-------
             ::  :    :* ::     *:  *   * :.***:*      : .

Sc      ----LQVNTNSRLKKWLRIYGWNASLTTLICIVVIFKRG-YIPYDVLKT-----SLSMTQ
Cg      NAKAERASTKKSLYLWLRVYGLNAALTTWICIVVILYRG-YYPFTLDASRIAGTKLEVRD
Ca      ----NRRVLDVNYYLWSIIYGFNAGFTTFVCLIWLII-E-YKNF----------QLSDLQ
Hs      --------------KWIRTPAIIYSVHTMTTLIPILSTFLFEDFSKASGFKGQRPETLHE
Mm      --------------RWIRIPAIIYAAHTITTLIPILYTLLFEDFSKAVAFKGQRPESFRE
Dr      --------------KWIRTPAIIYSVHVATTLVPILSHILFHKFPLSP---HPGPQTLNE
                      *    .   .   .   :: ::    :  :              :

Sc      KCQLASVYLPTFLIPLRLCFV*-----------------------
Cg      TLALMGLYLPTFLLPLRLCMLQQ----------------------
Ca      LINLLAIYIPYLLLPLILLIHSFKQIQ-QYNNNNHN---KLKQQ-
Hs      RLTLVSVYAPYLLIPFILLIFMLRSPYYKYEEKRKKK--------
Mm      RLTLVGVYAPYLIIPLILLLFMLRNPYYKYEEKRKKK--------
Dr      RLTLVSIYAPYLIIPIMILLTMLFSATYNSPSLKGNAPSKAKKQR
           * .:* * :::*: : :
```

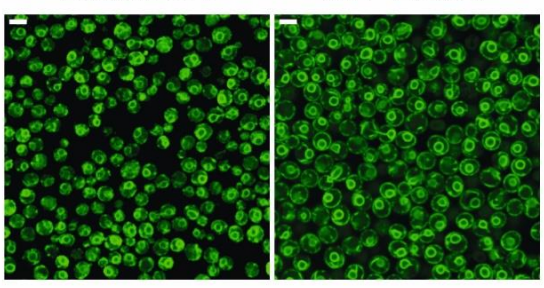

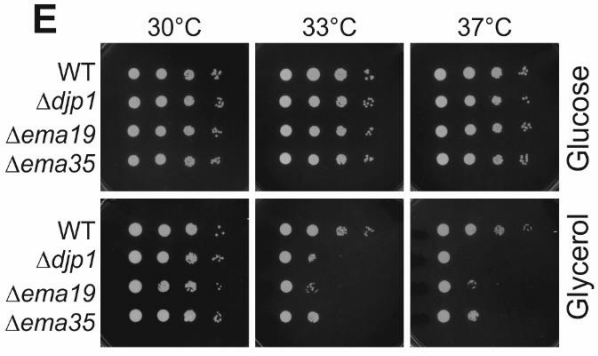

Fig. S2. Ema19 is highly conserved in eukaryotes. (A) Predicted localizations and membrane topologies of Ema17, Ema19 and Ema35. **(B)** Phylogenetic tree of Ema19 family members. **(C)** Alignment of Ema19; Sc, *Saccharomyces cerevisiae*; Cg, *Candida glabrata* KTA97029.1; Ca, *Candida albicans* EEQ46884.1; Hs, *Homo sapiens* AIC51228.1; Mm, *Mus musculus* NP_598467.1; Dr, *Danio rerio* XP_697605. **(D)** Ema19-GFP and GFP-Ema19 show the perinuclear staining characteristic for ER proteins. **(E)** *Δdjp1*, *Δema19* and *Δema35* mutants show a reduced growth on respiratory (glycerol) media at elevated temperatures.

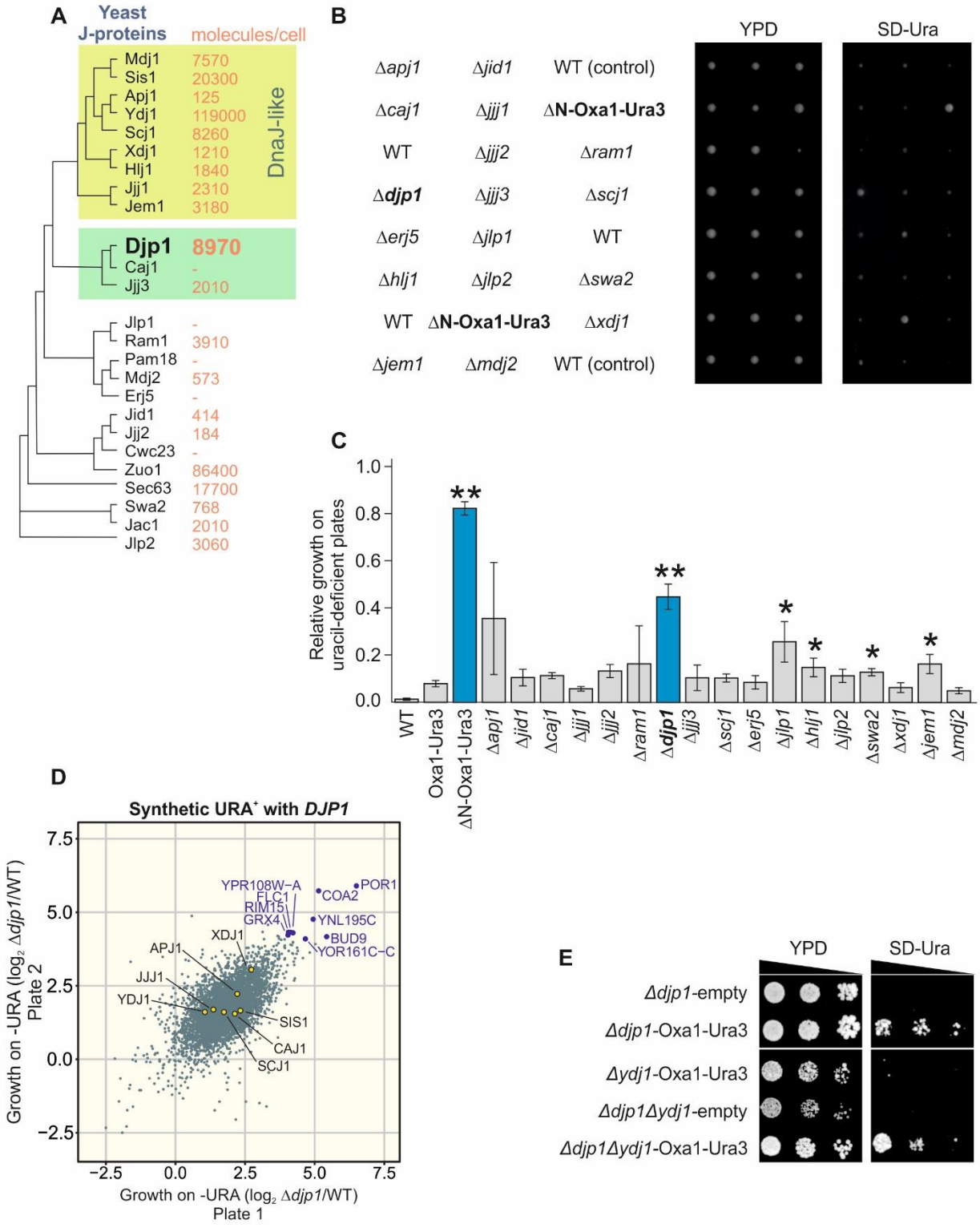
A
Yeast J-proteins
molecules/cell
Mdj1 7570
Sis1 20300
Apj1 125
Ydj1 119000
Scj1 8260
Xdj1 1210
Hlj1 1840
Jjj1 2310
Jem1 3180
DnaJ-like
Djp1 8970
Caj1 -
Jjj3 2010
Jlp1 -
Ram1 3910
Pam18 -
Mdj2 573
Erj5 -
Jid1 414
Jjj2 184
Cwc23 -
Zuo1 86400
Sec63 17700
Swa2 768
Jac1 2010
Jlp2 3060
B
YPD
SD-Ura
Δapj1 Δjid1 WT (control)
Δcaj1 Δjjj1 ΔN-Oxa1-Ura3
WT Δjjj2 Δram1
Δdjp1 Δjjj3 Δscj1
Δerj5 Δjlp1 WT
Δhlj1 Δjlp2 Δswa2
WT ΔN-Oxa1-Ura3 Δxdj1
Δjem1 Δmdj2 WT (control)
C
Relative growth on uracil-deficient plates
1.0
0.8
0.6
0.4
0.2
0.0
**
**
*
*
*
*
WT
Oxa1-Ura3
ΔN-Oxa1-Ura3
Δapj1
Δjid1
Δcaj1
Δjjj1
Δjjj2
Δram1
Δdjp1
Δjjj3
Δscj1
Δerj5
Δjlp1
Δhlj1
Δjlp2
Δswa2
Δxdj1
Δjem1
Δmdj2
D
Synthetic URA+ with DJP1
Growth on -URA (log2 Δdjp1/WT) Plate 2
Growth on -URA (log2 Δdjp1/WT) Plate 1
7.5
5.0
2.5
0.0
−2.5
−2.5
0.0
2.5
5.0
7.5
YPR108W-A
FLC1
RIM15
GRX4
POR1
COA2
YNL195C
BUD9
YOR161C-C
XDJ1
APJ1
JJJ1
YDJ1
SIS1
CAJ1
SCJ1
E
YPD
SD-Ura
Δdjp1-empty
Δdjp1-Oxa1-Ura3
Δydj1-Oxa1-Ura3
Δdjp1Δydj1-empty
Δdjp1Δydj1-Oxa1-Ura3

Fig. S3. Djp1 plays a unique role among the members of the J protein family. (A) Phylogenetic tree of the J proteins of *S. cerevisiae*. The sequences of the J proteins of yeast were aligned using Clustal Omega and a phylogenetic tree was calculated. The most abundant J protein, Ydj1, belongs to a group with highest similarity to the *E. coli* DnaJ protein. Djp1, Caj1 and Jjj3 form a sub-branch of the family, the function of which is largely elusive. Number of proteins per cell were reported by *(28).* **(B)** Growth phenotypes of the mutants indicated expressing Oxa1-Ura3 or ΔN-Oxa1-Ura3. WT with either Oxa1-Ura3 or ΔN-Oxa1-Ura3 was used as controls. (**C)** Quantification of the colony sizes in **(B).** The colony size of each mutant was first normalized to the growth on full media and afterwards compared to the negative control (Oxa1-Ura3). Shown is the mean of n=3 replicates ± standard deviation. *=$p<0.05$; **=$p<0.01$. **(D)** The growth rate of Oxa1-Ura3-expressing single yeast deletion mutants relative to *Δdjp1* double deletion mutants on uracil-deficient plates was systematically analyzed and quantified. *Δdjp1* Oxa1-Ura3 background was crossed into the deletion/DAmP library again to obtain double mutants, and their growth was tested on media lacking uracil. Simultaneous deletion of additional J proteins did not further increase the positive growth effect imposed by the absence of Djp1. On average, *Δdjp1* double mutants grew almost 4 times better than single mutants carrying the *DJP1* WT allele on SD-Ura media. **(E)** Simultaneous deletion of *Δdjp1* and *Δydj1* does not improve growth on media lacking uracil. Again, *Δydj1* did not accumulate Oxa1-Ura3 outside mitochondria.

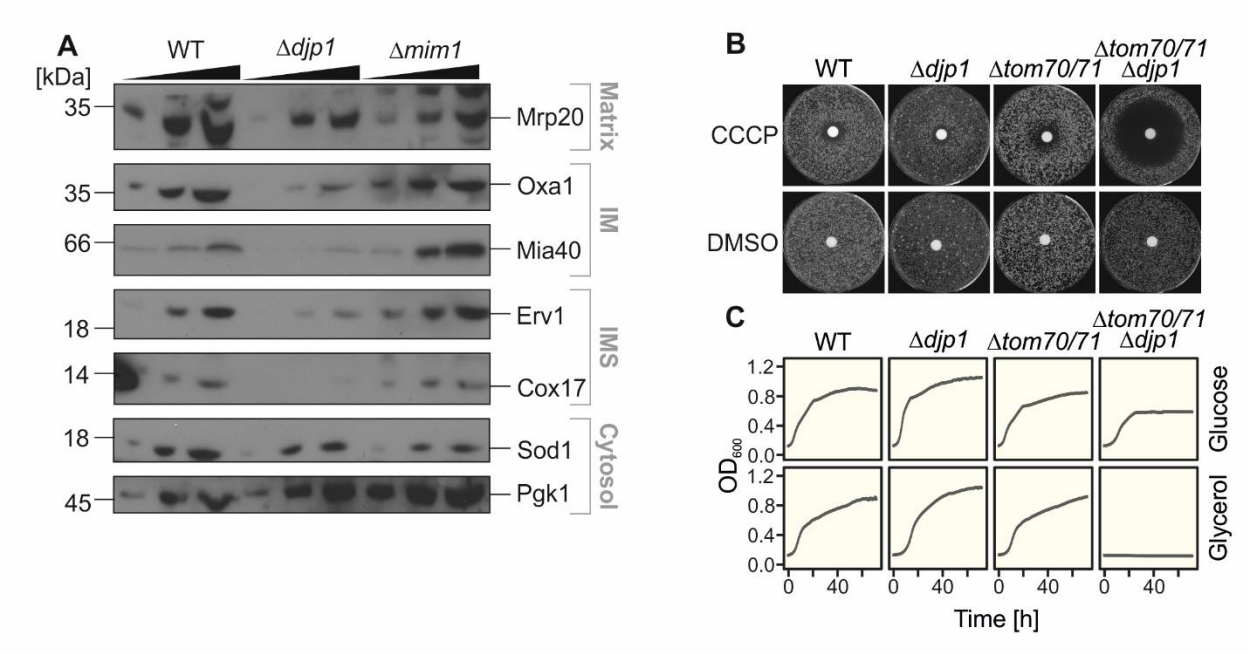

Fig. S4. In *Δdjp1* mutants, the presence of the TOM receptors Tom70/Tom71 are essential for respiration. (A) The strong reduction of mitochondrial protein levels in *Δdjp1* is not caused by an indirect effect via the Djp1 substrate Mim1. Increasing amounts of cell extracts (OD_{600} 0.1, 0.2, 0.4) were analyzed. **(B, C**) *Δtom70/71/Δdjp1* cells are hypersensitive to CCCP and unable to grow on the non-fermentable carbon source glycerol.

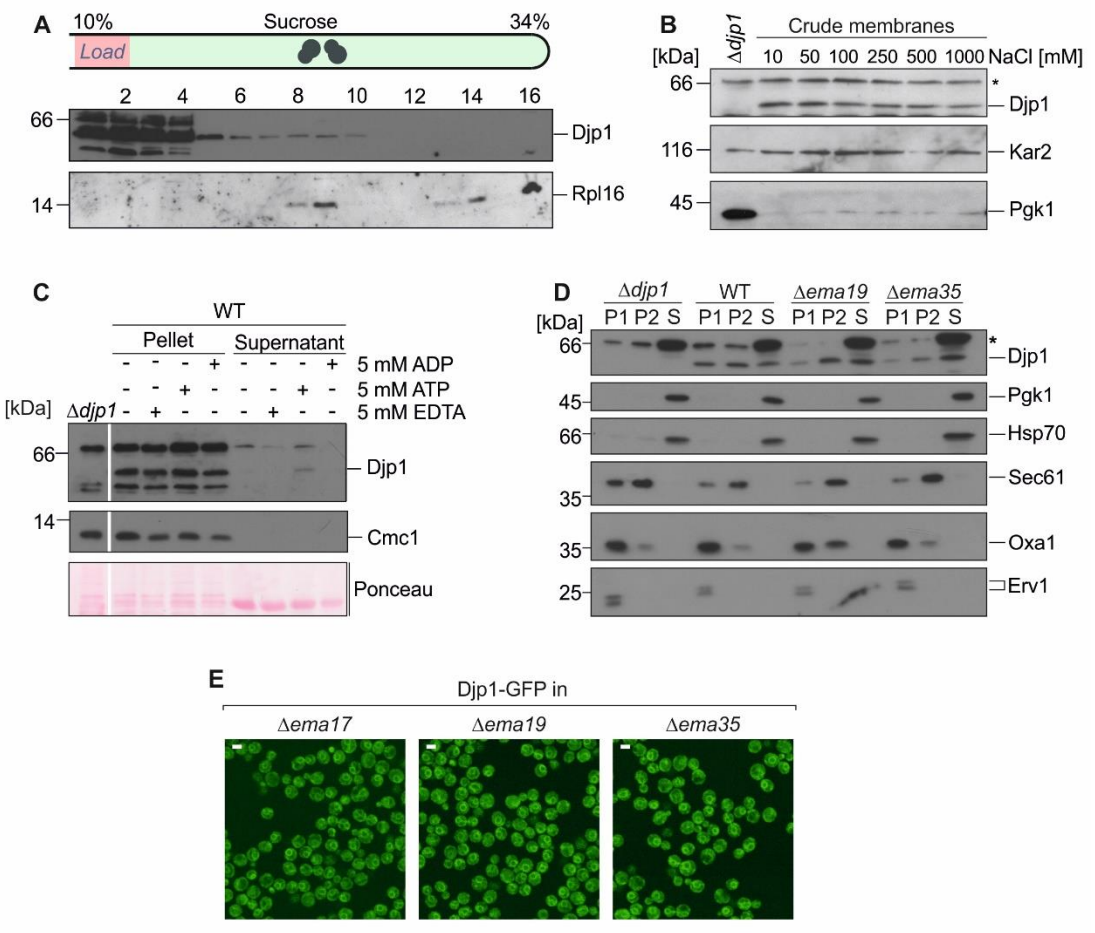

Fig. S5. Djp1 is bound to the ER surface. (A) Cellular extracts were separated by sucrose gradient centrifugation. Cytosolic ribosomes were mainly detected around fraction 9 and at the bottom of the gradient whereas Djp1 was almost exclusively found at the top of the gradient. There is no considerably co-migration of Djp1 with ribosomes. **(B)** Crude microsomal membranes were incubated with 0.6 M sorbitol, 20 mM Hepes, pH 7.5 and increasing amounts of NaCl. The membranes were reisolated and analyzed. Djp1 could not be removed from the membranes even upon washing with high concentrations of salt. **(C)** Microsomes were incubated with 100 mM NaCl, 0.6 M sorbitol and 20 mM Hepes pH 7.5 in the absence or presence of ADP, ATP or EDTA as indicated. Membranes were reisolated. Proteins in the membrane and supernatant fractions were analyzed by immune blotting. The membrane-binding of Djp1 was independent of nucleotides. **(D)** Membrane fractionation of *Δdjp1* and WT (as also shown in Fig. 2I), *Δema19* and *Δema35*. Yeast were homogenized and the different membranes were separated by differential centrifugation resulting in a pellet with enriched mitochondrial (P1) and a pellet (P2) with enriched ER membranes. The supernatant (S) containing the cytosolic fraction was precipitated. Oxa1 and Erv1 were used as mitochondrial control, Sec61 as an ER control, Hsp70 and Pgk1 were used as a cytosolic control. Djp1 is distributed between mitochondrial, ER and cytosolic fractions. In *Δema19* and *Δema35* this distribution appears to be shifted to the ER and the cytosol. **(E)** Fluorescence microscopy of Djp1-GFP in *Δema17*, *Δema19* and *Δema35* mutants. Scale bars, 5 µm. Djp1-GFP shows in all mutants a perinuclear staining.

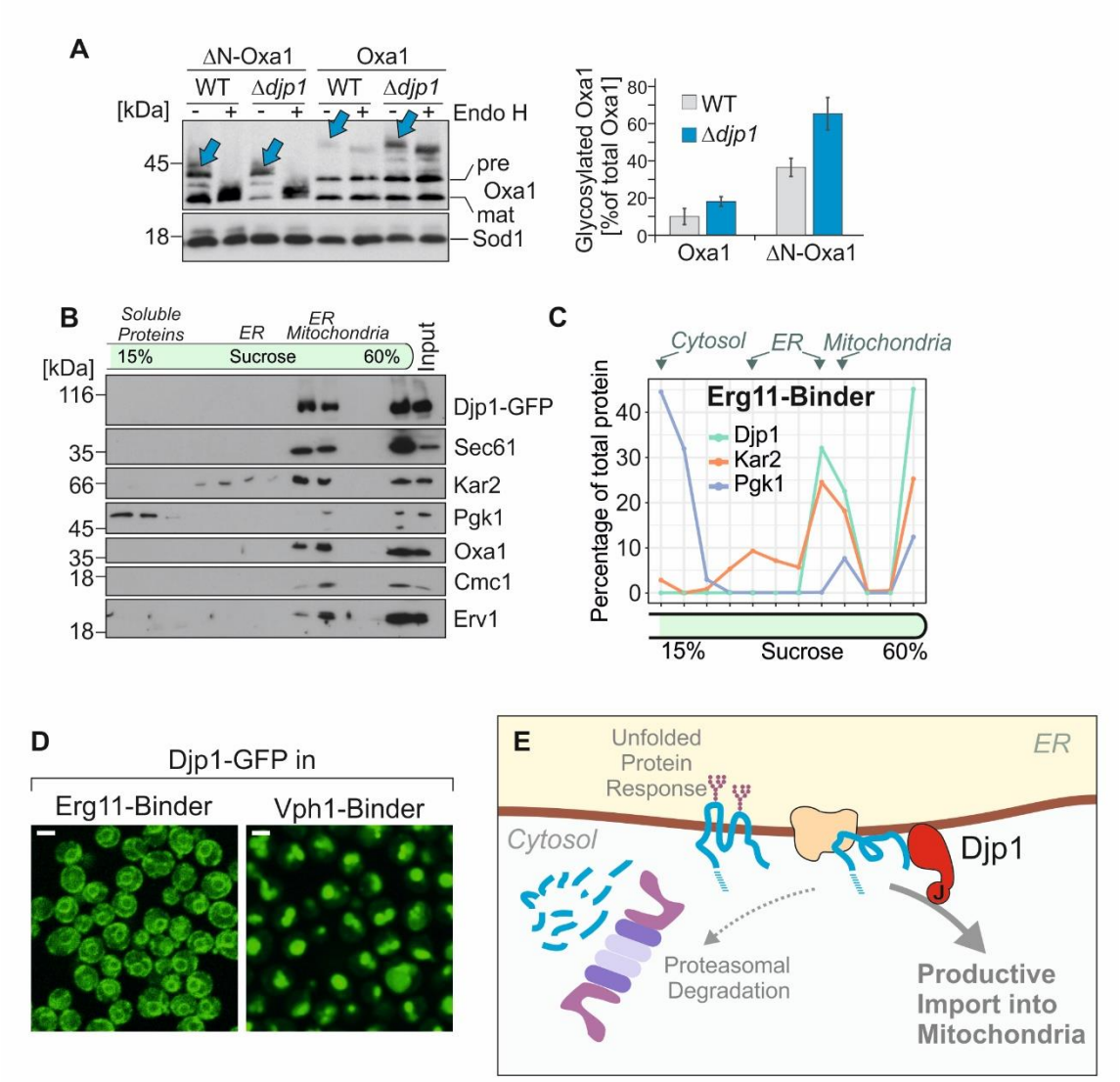

Fig. S6. Chromobody-based fusion proteins trap Djp1-GFP at different cellular localizations. (A) Whole cell lysates of yeast strains expressing Oxa1 or ΔN-Oxa1 from a *GAL*-promotor. A fraction of Oxa1 is glycosylated in *Δdjp1* cells (arrows), particularly if Oxa1 is expressed without presequence. The graph shows means ± standard deviation; n=3. **(B)** A membrane fraction of Djp1-GFP and Erg11-binder expressing cells was loaded onto a sucrose step gradient and centrifuged. The same volume of each fraction was analyzed by immune blot and decorated for mitochondrial (Erv1, Cmc1, Oxa1), ER (Sec61, Kar2) and cytosolic proteins (Pgk1) as well as against Djp1-GFP to visualize the distribution of the different organelles in the gradient. **(C)** The signals of panel B were quantified. Djp1-GFP is trapped at the ER membrane. **(D)** Fluorescence microscopy of Djp1-GFP co-expressed with Erg11- or Vph1-binder. Djp1-GFP shows perinuclear staining if co-expressed with Erg11-binder whereas the co-expression with Vph1-binder leads to a vacuolar staining. Scale bars, 5 µm. **(E)** Djp1 counteracts the proteasomal degradation of ER-bound Oxa1 precursor.

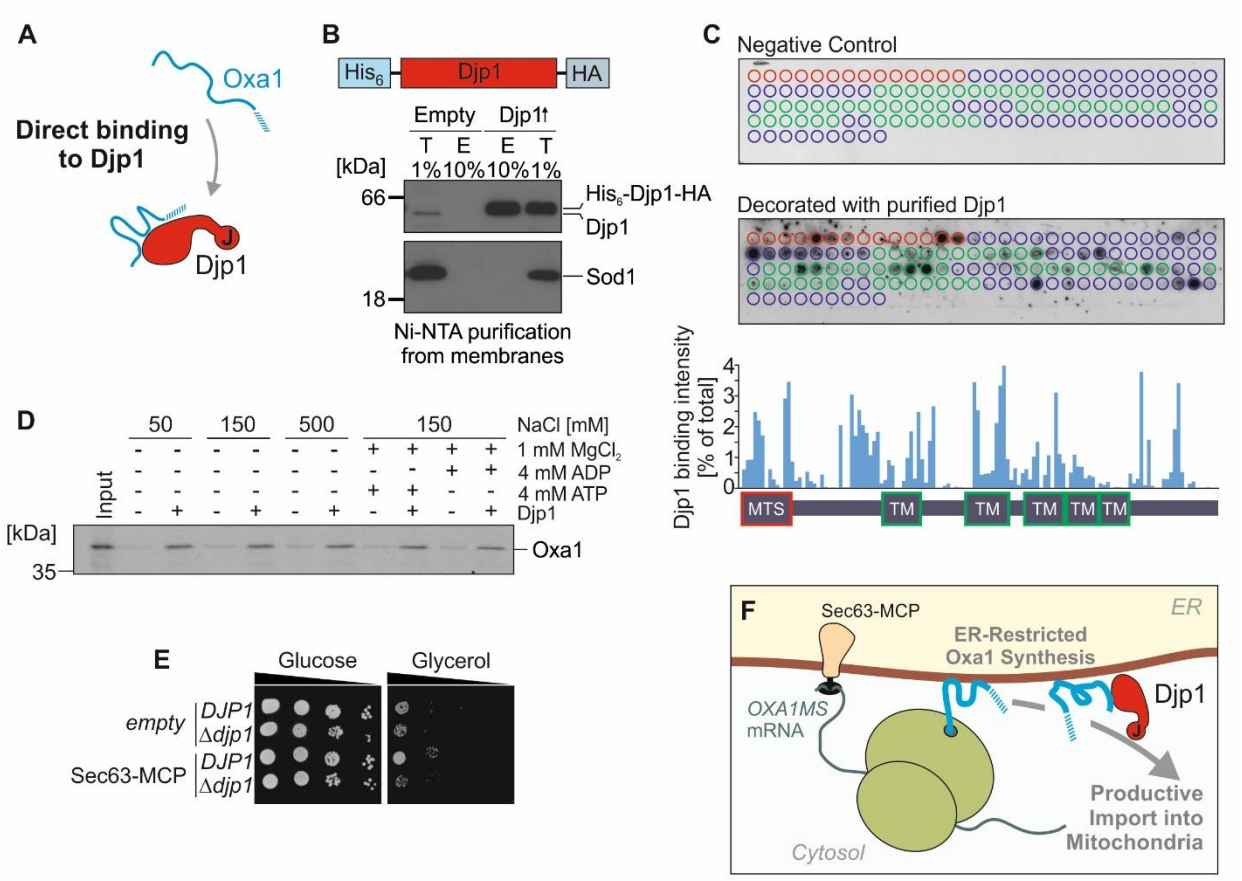

Fig. S7.Djp1 interacts directly with Oxa1. (A) In vitro binding experiments with recombinant Djp1. **(B)** His_6-Djp1-HA can be efficiently purified from membranes by Ni-NTA purification, shown is a test immune blot of the purification. Total (T) and elution (E) were loaded. As a control, membrane fractions of a yeast strain expressing an empty plasmid were used for purification. **(C)** 20mer peptides of the Oxa1 sequence, each shifted by three residues, were bound to a nylon membrane. The membrane was incubated with or without 1 µM purified HA-tagged Djp1 for 3 h. After extensive washing, the bound Djp1 was detected by immune blotting using HA-specific antibodies for both membranes. The Oxa1 sequences representing the mitochondrial targeting sequence (MTS) and the transmembrane domains (TM) are shown as red or green circles, respectively. Quantified signals of the membrane that was probed with Djp1 are shown on the bottom. Djp1 predominantly binds to regions upstream of the first transmembrane domain of Oxa1. **(D)** Oxa1 binds to Djp1-bound but not to empty sepharose beads. Djp1 was purified from yeast cells using affinity chromatography. Djp1-bound or empty sepharose beads were incubated with radiolabeled Oxa1 in presence of increasing amounts of salt and addition of $MgCl_2$, ATP or ADP as indicated. **(E, F)** An MS2 aptamer mRNA-binding motif (*9*) was introduced into the *OXA1 mRNA*. Upon expression of the MS2-binding fusion-protein Sec63-MCP, this mRNA is tethered to the ER, thereby restricting the translation of Oxa1 to the ER surface. The growth of yeast strains with ER-restricted synthesis of Oxa1 was tested on different carbon sources (glucose and glycerol) at 30°C. Djp1 is critical for mitochondrial respiratory functionality if Oxa1 synthesis occurs exclusively on the ER surface.

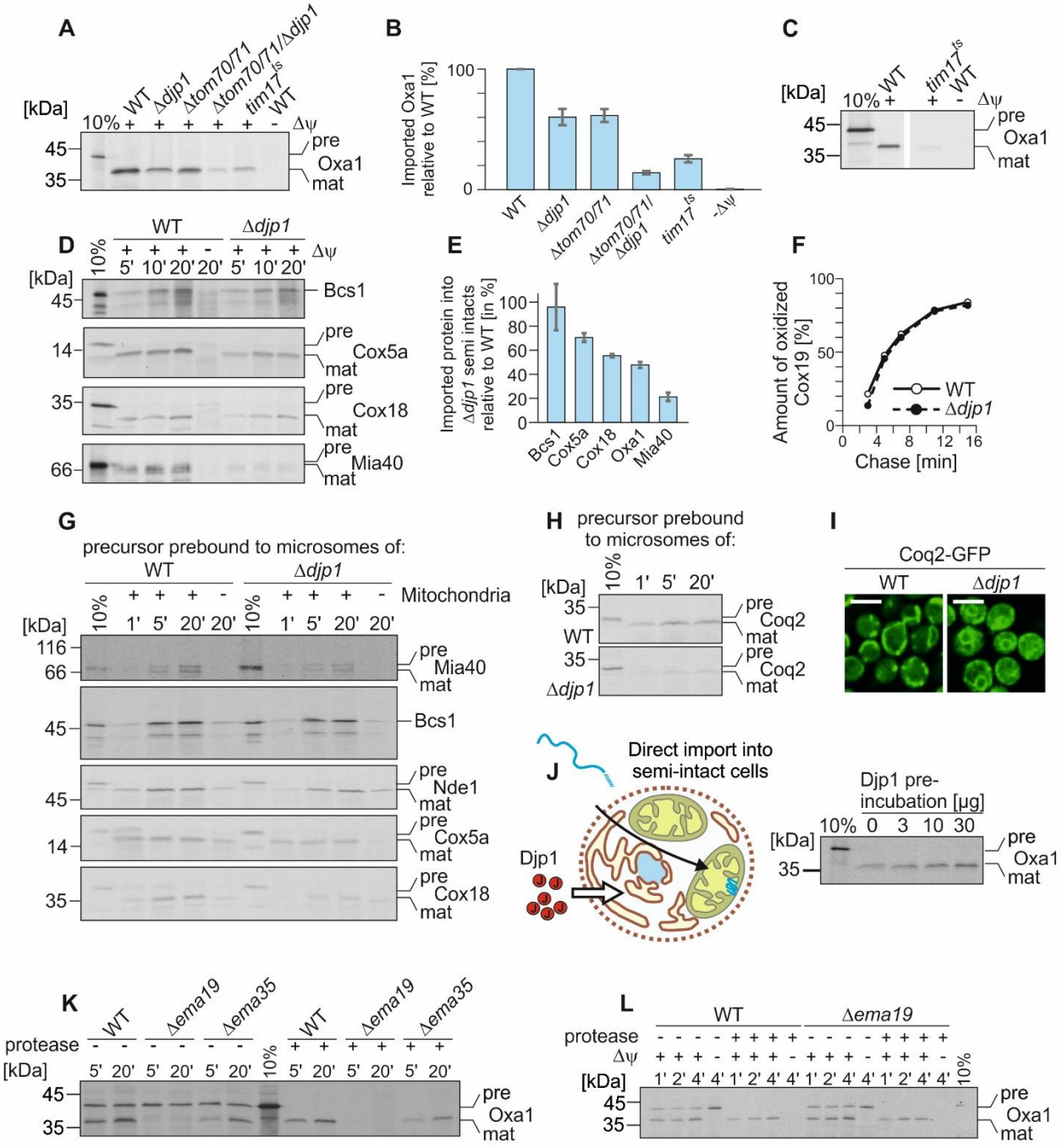
A
[kDa]
10%
WT
Δdjp1
Δtom70/71
Δtom70/71/Δdjp1
tim17ts
WT
Δψ
45
35
pre
Oxa1
mat
B
Imported Oxa1 relative to WT [%]
100
0
WT
Δdjp1
Δtom70/71
Δtom70/71/ Δdjp1
tim17ts
-Δψ
C
[kDa]
10%
WT
tim17ts
WT
Δψ
45
35
pre
Oxa1
mat
D
WT
Δdjp1
10%
5' 10' 20' 20' 5' 10' 20'
Δψ
[kDa]
45
Bcs1
14
pre
Cox5a
mat
35
pre
Cox18
mat
66
pre
Mia40
mat
E
Imported protein into Δdjp1 semi intacts relative to WT [in %]
100
80
60
40
20
0
Bcs1
Cox5a
Cox18
Oxa1
Mia40
F
Amount of oxidized Cox19 [%]
100
50
0
WT
Δdjp1
0
4
8
12
16
Chase [min]
G
precursor prebound to microsomes of:
WT
Δdjp1
Mitochondria
10%
1' 5' 20' 20'
[kDa]
116
66
pre
Mia40
mat
45
Bcs1
45
pre
Nde1
mat
14
pre
Cox5a
mat
35
pre
Cox18
mat
H
precursor prebound to microsomes of:
10%
1' 5' 20'
[kDa]
35
WT
pre
Coq2
mat
35
Δdjp1
pre
Coq2
mat
I
Coq2-GFP
WT
Δdjp1
J
Direct import into semi-intact cells
Djp1
Djp1 pre-incubation [μg]
10% 0 3 10 30
[kDa]
35
pre
Oxa1
mat
K
WT
Δema19
Δema35
WT
Δema19
Δema35
protease
[kDa]
5' 20' 5' 20' 5' 20' 10% 5' 20' 5' 20' 5' 20'
45
35
pre
Oxa1
mat
L
WT
Δema19
protease
Δψ
[kDa]
1' 2' 4' 4' 1' 2' 4' 4' 1' 2' 4' 4' 1' 2' 4' 4' 10%
45
35
pre
Oxa1
mat

Fig. S8. The relevance of Djp1 for mitochondrial import is not restricted to Oxa1. (A, B) Radiolabeled Oxa1 was imported into semi-intact cells of different mutants for 10 min. The import was quantified relative to the WT. Data shown are means ± standard deviations, n=3.The Oxa1 import in semi-intact cells depends on a functional translocation machinery and the membrane potential. **(C)** Radiolabeled Oxa1 was imported into isolated WT and temperature-sensitive *tim17* mutant mitochondria. All samples were treated with protease. Like in the experiment with semi-intact cells, import into isolated mitochondria required functional import components and energized mitochondria. **(D)** Radiolabeled precursor proteins were imported into semi-intact cells of WT or *Δdjp1*. Samples were taken after the indicated time points and non-imported protein was removed by protease treatment. **(E)** The indicated proteins were imported into semi-intact cells for 20 min as described for panel **D**. Signals were quantified. Data shown are means ± standard error, n≥3. Besides Bcs1, the import of all here tested precursor proteins was Djp1-dependent. **(F)** WT and *Δdjp1* cells were pulse labeled for 3 min. Radiolabeling was stopped. After different times (chase), the Mia40 substrate Cox19 was precipitated and its redox state analyzed by alkylation. The oxidation rates and thus the import of this soluble IMS protein was not affected by the absence of Djp1. **(G, H)** Mitochondrial precursor proteins were radiolabeled and pre-bound to microsomes. Microsomes were reisolated and incubated with WT mitochondria as indicated. All samples were protease-treated to show only imported proteins. Djp1 was critical for the ER-to-mitochondria hand-over of the membrane proteins Mia40, Cox18 and Coq2. **(I**) Coq2-GFP in *Δdjp1* cells shows a mixed population of cells with many demonstrating ER staining. Scale bars, 5 µm. **(J)** Semi-intact cells were preincubated with different amounts of purified Djp1, as indicated, followed by a direct import of Oxa1. The import efficiency was increasing with the increasing amounts of Djp1 added. **(K)** Oxa1 was imported into semi-intact cells of WT, *Δema19* and *Δema35*. Only low amounts of Oxa1 were imported into *Δema19* mitochondria in semi-intact cells. **(L)** Oxa1 was imported into WT and *Δema19* mitochondria. There is no difference in the import kinetics when isolated mitochondria are used.

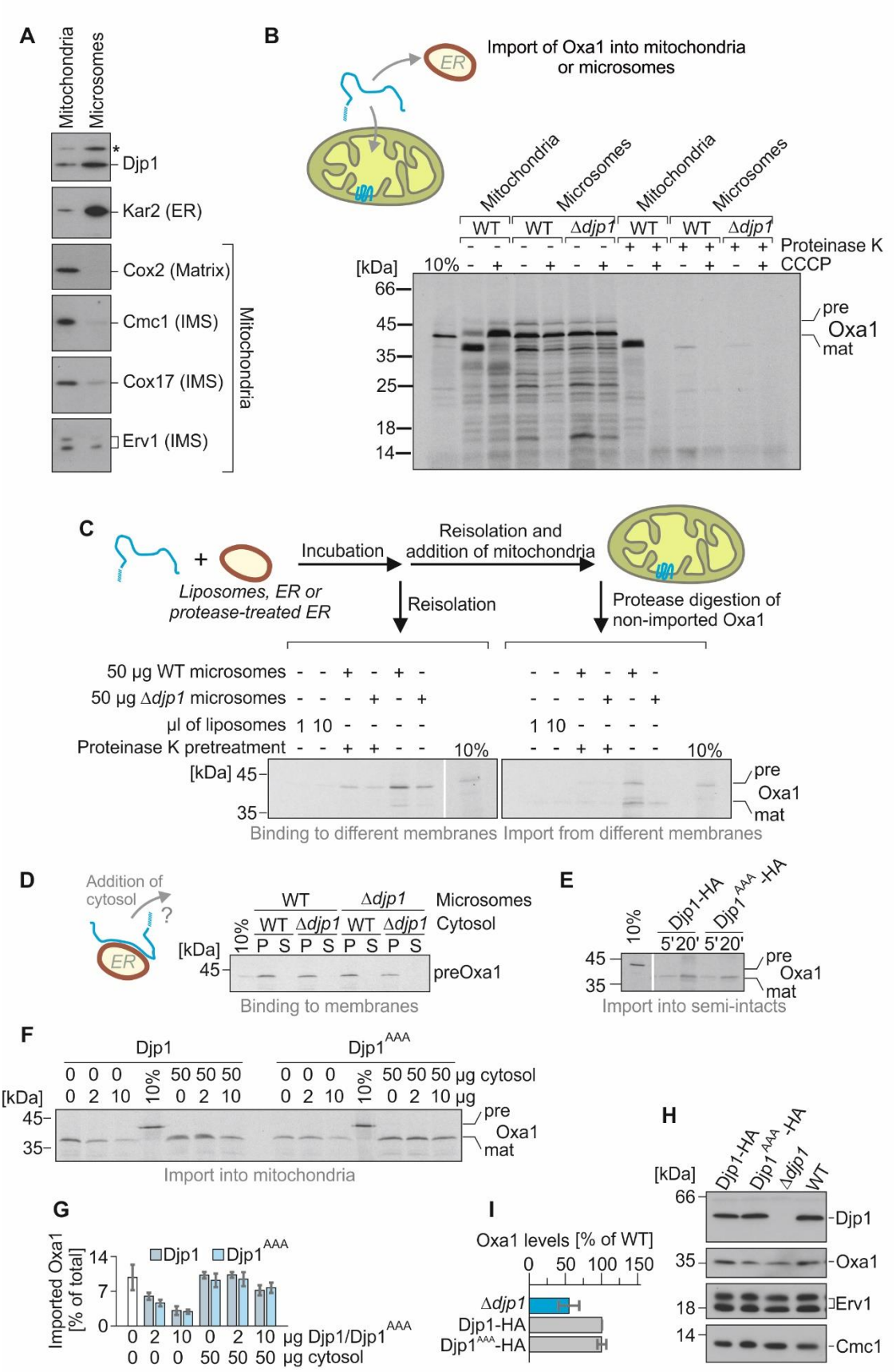

Fig. S9. Djp1 facilitates the hand-over of Oxa1 precursors from the ER surface to mitochondria. (A) Protein levels in mitochondrial and microsomal fractions isolated from

yeast cells. A non-specific signal of the Djp1 antibody is indicated by an asterisk. Djp1 is enriched in isolated microsomes. **(B)** Oxa1 is imported into mitochondria but not into microsomes. Oxa1 was incubated with mitochondria or microsomes for 30 min in absence or presence of CCCP. To test the amount of integrated Oxa1 in the different organellar membranes, half of the samples were protease treated to remove free Oxa1 precursor. **(C)** Oxa1 was incubated with either liposomes, protease-treated microsomes or microsomes. After reisolation of the membranes, the amounts of Oxa1 bound to these membranes was analyzed. Moreover, these membranes were mixed with mitochondria and the amounts of imported Oxa1 protein was analyzed after 20 min. The binding of Oxa1 to the ER membrane as well as its hand-over to mitochondria was Djp1-dependent. **(D)** Oxa1 was incubated with microsomes. The membranes were reisolated and incubated with cytosol of WT or *Δdjp1*. The membranes were pelleted (P) and the proteins of the supernatant (S) were precipitated. Oxa1 remained completely microsome-bound. Even in the presence of Djp1, it was not released into the cytosol. **(E)** Oxa1 precursor was imported into semi-intact Djp1-HA and Djp1^{AAA}-HA cells. Samples were protease-treated to show imported Oxa1. The J domain of Djp1 is not necessary for efficient Oxa1 import into mitochondria of semi-intact cells. **(F, G)** Radiolabeled Oxa1 precursor was preincubated with different concentrations of isolated Djp1 in the absence or presence of yeast cytosol for 5 min before *Δdjp1* mitochondria were added. Non-imported protein was removed by protease treatment. Mean values and standard errors of three experiments are shown. The addition of cytosol did not increase the import of Oxa1. Preincubation with purified Djp1 did decrease the import independent of a functional J domain. **(H, I)** Levels of the indicated proteins were detected by immune blotting of cell extracts and quantified from three independent experiments. Shown are mean values and standard errors. The steady state levels of Oxa1 are not changed in the Djp1^{AAA}-HA mutant.

References

20. Y. Cohen, M. Schuldiner, Advanced methods for high-throughput microscopy screening of genetically modified yeast libraries. *Methods Mol Biol* **781**, 127-159 (2011).
21. A. Ramesh *et al.*, A disulfide bond in the TIM23 complex is crucial for voltage gating and mitochondrial protein import. *J Cell Biol* **214**, 417-431 (2016).
22. I. Yofe *et al.*, One library to make them all: streamlining the creation of yeast libraries via a SWAp-Tag strategy. *Nat Methods* **13**, 371-378 (2016).
23. C. Janke *et al.*, A versatile toolbox for PCR-based tagging of yeast genes: new fluorescent proteins, more markers and promoter substitution cassettes. *Yeast* **21**, 947-962 (2004).
24. M. J. Kuehn, J. M. Herrmann, R. Schekman, COPII-cargo interactions direct protein sorting into ER-derived transport vesicles. *Nature* **391**, 187-190 (1998).
25. N. Mesecke *et al.*, The zinc-binding protein Hot13 promotes oxidation of the mitochondrial import receptor Mia40. *EMBO Rep.* **9**, 1107-1113 (2008).
26. V. Peleh, E. Cordat, J. M. Herrmann, Mia40 is a trans-site receptor that drives protein import into the mitochondrial intermembrane space by hydrophobic substrate binding. *Elife* **5**, (2016).
27. C. Meisinger, N. Pfanner, K. N. Truscott, Isolation of yeast mitochondria. *Methods Mol Biol* **313**, 33-39 (2006).
28. S. Ghaemmaghami *et al.*, Global analysis of protein expression in yeast. *Nature* **425**, 737-741 (2003).